Deep-Sea Research I 57 (2010) 368–383

Contents lists available at ScienceDirect

Deep-Sea Research I

journal homepage: www.elsevier.com/locate/dsri

Interactive effects of iron, irradiance and CO_2 on Ross Sea phytoplankton

Y. Feng [a], C.E. Hare [a], J.M. Rose [a,i], S.M. Handy [a], G.R. DiTullio [b,c], P.A. Lee [c], W.O. Smith Jr. [d], J. Peloquin [d,j], S. Tozzi [d,k], J. Sun [e], Y. Zhang [a], R.B. Dunbar [f], M.C. Long [f], B. Sohst [g], M. Lohan [l], D.A. Hutchins [h,*]

[a] College of Marine and Earth Studies, University of Delaware, Lewes, DE, USA
[b] Hollings Marine Lab, College of Charleston, Charleston, SC 29412, USA
[c] Grice Marine Laboratory, College of Charleston, Charleston, SC 29412, USA
[d] Virginia Institute of Marine Sciences, Gloucester Pt., VA 23062, USA
[e] Institute of Oceanology, Chinese Academy of Sciences, Qingdao, China
[f] Environmental Earth System Science Department, Stanford University, Stanford, CA, USA
[g] Old Dominion University, Norfolk, VA, USA
[h] Department of Biological Sciences, University of Southern California, Los Angeles, CA, USA
[i] Biology Department, Woods Hole Oceanographic Institution, Woods Hole, MA, USA
[j] Institute of Biogeochemistry and Pollutant Dynamics, ETH Zürich, Zürich, Switzerland
[k] Monterey Bay Aquarium Research Institute, 7700 Sandholdt Road, Moss Landing, CA, USA
[l] School of Earth, Ocean and Environmental Sciences, University of Plymouth, Plymouth PL4 8AA, United Kingdom

ARTICLE INFO

Article history:
Received 15 May 2009
Received in revised form
23 October 2009
Accepted 18 November 2009
Available online 26 November 2009

Keywords:
CO_2
Irradiance
Iron limitation
Phytoplankton
Diatoms
Phaeocystis
Ross Sea
Global change
Co-limitation
Interactive effects
Southern Ocean

ABSTRACT

We conducted a factorial shipboard continuous culture experiment to examine the interactive effects of altered iron, irradiance and CO_2 on the summer phytoplankton community of the Ross Sea, Antarctica. After 18 days of continuous incubation, iron enrichment increased phytoplankton biomass, nutrient drawdown, diatom and *Phaeocystis* abundance, and some photosynthetic parameters. High irradiance significantly increased the number of *Phaeocystis antarctica* colonies, as well as *P. antarctica* abundance relative to diatoms. Iron and light had significant interactive effects on diatom and *P. antarctica* pigment concentrations, *P. antarctica* colony abundance, and Si:N, Si:C, and N:P ratios. The major influence of high CO_2 was on diatom community structure, by favoring the large centric diatom *Chaetoceros lineola* over the small pennate species *Cylindrotheca closterium*. The ratio of centric to pennate diatoms was significantly responsive to changes in all three variables individually, and to all of their possible two- and three-way combinations. These results suggest that shifts in light, iron, and CO_2 and their mutual interactions all play a role in controlling present day Ross Sea plankton community structure, and need to be considered when predicting the possible future responses of biology and biogeochemistry in this region.

1. Introduction

The Southern Ocean plays an important role in modulating the global climatic system by transporting and storing heat, fresh water, nutrients, and anthropogenic CO_2 (Lovenduski and Gruber, 2005). This area is likely to be greatly influenced by global change, since polar marine ecosystems are particularly sensitive (Sarmiento and Toggweiler, 1984, Sarmiento et al., 1998), and small temperature differences can have large effects on the extent and thickness of sea ice (Smetacek and Nicol, 2005). In fact, some parts of the Southern Ocean such as the coastal Antarctic Peninsula are among the fastest warming regions on the planet (Vaughan et al., 2003). The biological communities of the Peninsula region have been dramatically impacted by the changes in ice cover that have occurred over the past 3 decades (Montes-Hugo et al., 2009). Recent data now suggest that a 50 yr warming trend extends over all of western Antarctica, including the Ross Sea (Steig et al., 2009).

There are two main dominant phytoplankton taxa in the Ross Sea (DiTullio and Smith, 1996; Arrigo et al., 1999, 2000; Smith and Asper, 2001). One is the diatoms, which regulate the silicon cycle in the ocean (Tréguer et al., 1995), and are important in supporting most krill-based food webs in the Antarctic (Knox, 1994). These include weakly silicified, fast-growing diatom species as well as larger, grazer-resistant, heavily silicified ones (Smetacek and Nicol, 2005). The prymnesiophyte *Phaeocystis antarctica* is another major taxon. This species strongly influences the marine biogeochemical cycles of carbon and nutrients and has significantly higher C:P and N:P ratios than diatoms (Jennings et al., 1984; Karl et al., 1991; Ishii et al., 1998; Bates et al., 1998;

* Corresponding author.
E-mail address: dahutch@usc.edu (D.A. Hutchins).

0967-0637/$ - see front matter © 2009 Elsevier Ltd. All rights reserved.
doi:10.1016/j.dsr.2009.10.013

Rubin et al., 1998; Takeda, 1998; Arrigo et al., 2000; Sweeney et al., 2000). *Phaeocystis* is also a major source of the climatically important gas dimethylsulfide (DMS) through its prolific production of dimethylsulfoniopropionate (DMSP) (Gibson et al., 1990; DiTullio and Smith, 1995; DiTullio et al., 2000). Assemblage dominance by this colony-forming prymnesiophyte has additional implications for food web structure, since colonial *Phaeocystis* are not preferred by most Antarctic meso- and microzooplankton grazers (Verity and Smetacek, 1996; Smith et al., 2003; Haberman et al., 2003a, b). The relative dominance of diatoms and *Phaeocystis* in Ross Sea phytoplankton communities may play a significant role in shaping its food web and the biogeochemical cycles of carbon, sulfur, and nutrients. Therefore, it is critical to understand the possible responses of these two functional groups to future global changes (Smith et al., 2000).

It has been established that irradiance (e.g. mixed layer depth, Mitchell and Holm-Hansen (1991); Nelson and Smith (1991)) and iron availability (Timmermans et al., 2001) are two of the main factors affecting phytoplankton dynamics in the Southern Ocean. In particular, mixed layer depth (MLD) has been suggested to determine the dominant species in the Ross Sea area. *P. antarctica* often dominates in areas with deeper MLD (DiTullio and Smith, 1996; Arrigo et al., 1999, 2000; Sweeney et al., 2000; Smith and Asper, 2001), consistent with the high photosynthetic and quantum efficiency of *P. antarctica* cells under low-light conditions (Moisan et al., 1998; Moisan and Mitchell, 1999). Diatoms are usually most abundant in areas of shallower MLD and more stratified waters (DiTullio and Smith, 1996; Arrigo et al., 1999). Both C:P and N:P drawdown ratios and new production rates of *P. antarctica* are much higher than those of diatoms. Thus, it is possible that any shift away from *P. antarctica* and towards diatoms in response to global warming-enhanced upper ocean stratification could decrease carbon export to sub-euphotic depths (Arrigo et al., 1999).

Iron availability is another important factor that influences phytoplankton biomass and taxonomic composition in the Southern Ocean. Martin et al. (1990a, b) proposed that the productivity in the Southern Ocean was limited by iron availability. Results of many shipboard iron enrichment studies (Martin et al., 1990b; Takeda, 1998; Boyd et al., 1999; Hutchins et al., 2001) and *in situ* experiments (Boyd et al., 2000; Gervais et al., 2002; Coale et al., 2004) all confirmed that iron supply could control the growth of phytoplankton in the Southern Ocean.

Some iron-addition experiments (Boyd et al., 2000; Nodder et al., 2001; Strass, 2002) found large diatom blooms after iron enrichments. Other work also indicated that *Phaeocystis* may be iron limited in the Ross Sea (Olson et al., 2000) and may need more iron than diatoms to bloom (Coale et al., 2003; Sedwick et al., 2008). Hutchins et al. (2002) also found a shift from the solitary stage of *P. globosa* to the colonial form after iron enrichment in the offshore northern Humboldt Current. The relative responses of diatoms and *Phaeocystis* to changes in iron availability such as those resulting from melting sea ice (Sedwick and DiTullio, 1997) remain an uncertain aspect of the ecological competition between the two groups.

Some research has suggested that CO_2 concentrations may be important in structuring algal assemblages as well (Tortell et al., 2002, 2008; Feng et al., 2009), due at least in part to species-specific differences in the physiological mechanisms of inorganic carbon acquisition. Diatoms are closer to CO_2 saturation than *Phaeocystis* at current CO_2 concentrations due to their different carbon acquisition mechanisms (Riebesell, 2004). Therefore, the growth of diatoms would not be expected to be easily limited by CO_2 availability, while *Phaeocystis* could potentially be more vulnerable to CO_2 limitation. *Phaeocystis* colonies may also be at a disadvantage in obtaining dissolved CO_2 compared to generally smaller diatom cells due to diffusion limitation constraints. In light of the projected end of the century atmospheric pCO_2 of 700–800 μatm (Alley et al., 2007), these differences could have important implications for phytoplankton community structure as well. These few studies suggest the possibility of a CO_2-driven shift towards increased *Phaeocystis* dominance in the future high CO_2 Southern Ocean.

The extent to which irradiance, iron, and CO_2 individually and together influence the balance between diatoms and *Phaeocystis* in this region remains poorly understood. Indeed, these three environmental factors are not independent of each other, and synergistic or antagonistic interactions on biological processes almost certainly occur. Iron-light co-limitation has long been recognized as a potential issue in the Southern Ocean, since deep mixed layers and seasonally low irradiance coupled with low iron concentrations are common throughout much of the area (Sunda and Huntsman, 1995; Boyd and Abraham, 2001; Boyd et al., 1999, 2001; de Baar et al., 2005; Blain et al., 2008; Hewes et al., 2008; Pollard et al., 2009). In other phytoplankton, such as coccolithophores and cyanobacteria, interactive effects have also been documented between CO_2 and irradiance availability (Feng et al., 2008), and between CO_2 and iron availability (Fu et al., 2008). These interactive effects among multiple global change variables can be non-linear, and thus difficult to accurately predict. Since mixed layer depth, iron availability, and pCO_2 will all likely change simultaneously with shifting climate regimes, understanding the combined influences of all three in the future Southern Ocean is as important as understanding each in isolation.

The Ross Sea is an excellent system to investigate the environmental factors that regulate the distribution and production of diatoms and *P. antarctica*. This area is characterized by seasonal blooms of both groups, which are typically separated in both space and time (DiTullio and Smith, 1996; Arrigo et al., 1999, 2000; Smith et al., 2000; Peloquin and Smith, 2007). Here we present the results of a set of shipboard manipulative experiments conducted during austral summer in the Ross Sea, in which we examined the individual and combined influences of light, iron, and pCO_2 on the balance between these two key functional groups, and on the biogeochemical cycles that they mediate.

2. Material and methods

2.1. Incubation system setup and sampling

We conducted a shipboard continuous incubation (Hutchins et al., 2003; Pickell et al., 2009) with a natural Ross Sea phytoplankton assemblage using an "Ecostat" system (Hare et al., 2005, 2007a, b). All parts of the system were built of Teflon or polycarbonate, and were rigorously acid cleaned prior to the experiment to ensure no potential trace-metal contamination. Near-surface water (~10 m, salinity 34.3, 0.1 °C) containing intact phytoplankton was collected at 74.23 °N, 179.23 °W on December 27, 2005. The depth of water collections corresponded approximately to the 15% light level, in between the 7% and 33% levels used in the low-light and high-light treatment incubators, respectively. Surface water pCO_2 was measured continuously using the underway equilibrator system installed on the ship; pCO_2 within 5 km of the collection location averaged 228 ± 20 μatm (unpublished data). The water was placed in a 50-L mixing carboy from a trace-metal clean, towed, Teflon diaphragm pumping system, similar to the one utilized by Bruland et al. (2005). In order to eliminate macrozooplankton, the water was cleanly filtered through acid-washed 200 μm Nitex mesh. Twenty-four acid-washed 2.7 L clear polycarbonate bottles

were used for the incubation. Trace-metal clean 0.2 μm in-line filtered seawater was also collected at the same time as the whole phytoplankton assemblage for use as dilution media during the continuous culture incubations. The initial nitrate, phosphate, silicic acid and dissolved iron concentrations in the collected seawater were 23.59, 1.53, 66.3 μM and 0.18 nM, respectively. The nutrient concentrations in the reservoirs were monitored frequently and there were no significant changes during the course of the incubation.

Two Ecostat incubator systems were used for the continuous incubation experiment. One was set up for the "low-light" (LL) treatment with an irradiance of ~7% of incident sea surface levels; the other was used for the "high-light" (HL) treatment at approximately 33% of sea surface irradiance. The irradiances were adjusted by covering the incubators with a combination of spectrally corrected blue plastic (Hutchins et al., 1998) and neutral density screens. Photosynthetically active radiation (PAR) reaching the incubators was measured continuously throughout the experiment using a BioSpherical Instruments QSR 2100 quantum meter calibrated prior to the cruise. Four iron and CO_2 treatments were examined at each irradiance: (1) unenriched control, 380 ppm CO_2 (control, low CO_2); (2) unenriched control, 750 ppm CO_2 (control, high CO_2); (3) 1 nM added iron ($FeCl_3$ in 0.01 N HCl), 380 ppm CO_2 (plus iron, low CO_2); and (4) 1 nM added iron, 750 ppm CO_2 (plus iron, high CO_2). Triplicate bottles were incubated for each of the eight iron/CO_2/light treatments, and results presented are the means and standard deviations of three separate samples, one from each triplicate.

The two pCO_2 levels were set by gentle bubbling (3 mL min^{-1}) of ambient air (~380 ppm CO_2) or a HEPA-filtered commercially prepared air/CO_2 mixture (760 ppm CO_2) into the incubation systems throughout the incubation. Ambient air was collected using an air pump with a HEPA-filtered intake near the ship's bow to avoid contamination. The carbonate system in the incubation system was monitored throughout the experiment using both pH and DIC measurements. The incubation temperature was maintained at 0 ± 1 °C using a circulating seawater bath, close to the natural surface seawater temperature of the collected water.

The incubation was carried out in "batch" growth mode during the first 5 days of incubation (T0–T5) to acclimate the phytoplankton to the experimental conditions and avoid "wash-out" during the initial lag period. The continuous incubation started on T5 and was maintained for 13 days until the final sampling day (T18). The dilution rate was set at 0.4 d^{-1}, adjusted by pumping 0.2 μm filtered seawater through inflow lines into the bottles from the top of the caps using 24 peristaltic pumps. This rate is within the range of published average phytoplankton growth rates in this area (Smith and Nelson, 1985).

The outflow was collected by gravity through Tygon tubing connected on the shoulders of incubation bottles, and drained into another set of 24 2.7 L polycarbonate bottles, which were stored in the dark. Only a small volume (less than 10%) of daily sampling was taken directly from the incubation bottles using clean syringes. These samples were used to measure Chl-*a*, dissolved nutrients, cell abundance via microscopy, pH, and dissolved inorganic carbon (DIC). Due to volume limitations, some of these samples were only taken on alternate days. Algal pigment composition by HPLC, particulate organic carbon (POC) and nitrogen (PON), particulate organic phosphorus (POP), and biogenic silica (BSi) were sampled from the outflow bottles. Previous works with the Ecostat system comparing bulk parameters and phytoplankton community structure in the bottles and in the outflow collections have found no significant differences between the two, as long as water collections are made at least every 24 h (Hare et al., 2005, 2007a, b). On the final day (T18), all of the parameters were sampled directly from the incubation bottles.

2.2. Seawater carbonate system measurements

Samples for total dissolved inorganic carbon (ΣCO_2) analysis were collected in 250 mL borosilicate glass bottles and poisoned with 50 μL saturated $HgCl_2$ solution immediately after sampling, in accordance with JGOFS protocols (Dickson and Goyet, 1994). Samples were warmed to room temperature (~20 °C) prior to analysis within 3–12 h of collection. DIC was measured by infrared absorption analysis of CO_2 evolved from acidified samples in a nitrogen carrier gas stream, using an automated system connected to an infrared gas analyzer (LI-COR LI7000). The system consists of a high-precision digital pump (Kloehn VersaPump 6), which delivers a precise volume of seawater to a small sparging tube; 0.1 mL of phosphoric acid (3 N) was added by a micropump and the sample bubbled with ultrahigh purity nitrogen equipped with an in-line CO_2 scrubber. Before entering the LI-COR infrared gas analyzer, the gas stream passes through a Nafion dryer and a magnesium perchlorate water trap. The gas flow is regulated precisely using a silicon orifice mass flow controller (Redwood Microsystems, MEMS-Flow Model 9900). Integrating the infrared absorbance signal with respect to time yields the total amount of CO_2 evolved from the sample. Integrations were performed using the LI-COR firmware. These peak-area measurements were calibrated using certified reference materials (CRMs) obtained from Andrew Dickson at UCSD-SIO. CRMs were analyzed as unknowns to constrain instrument drift due to water accumulation. Precision estimated on the basis of triplicate analysis of all unknown seawater samples was ± 1.2 μmol kg^{-1}. pCO_2 values were calculated from DIC and pH values (Mehrbach et al., 1973; Weiss, 1974).

High-precision pH was determined following the spectrophotometric method described in Dickson et al. (2003). Samples were taken directly from the incubation bottles and placed into 30 mL spectrophotometer cells, which were then sealed with rubber caps. The cells were placed in a temperature equilibrator and warmed to 25 °C over 30–45 min immediately after sample collection. The cells then were placed in a temperature controlled 10 cm path length holder (Ocean Optics scanning UV–vis–IR), and blank values were measured at 730, 578, and 434 nm. 50 μL of 2.2 mmol kg^{-1} m-Cresol purple dye was then injected into the cell through one of the end caps, and the absorbances were re-measured. pH was calculated from the absorbances and acid dissociation constants given in Dickson et al. (2003). Precision was better than ± 0.002 pH units.

2.3. Phytoplankton biomass and community composition analyses

Samples for total Chl-*a* measurements were filtered onto 0.2 μm polycarbonate filters (Millipore), extracted in 90% acetone at −20 °C in the dark for 18–24 h, and measured with a Turner 10-AU fluorometer (Welschmeyer, 1994). Phytoplankton samples for taxonomic identification were fixed with a final concentration of 1% gluteraldehyde and stored at 4 °C in darkness until analysis. Cell enumeration and identification were performed using an inverted transmitted light microscope (Leica DM IRBE) equipped with a Hamamatsu charge-coupled device camera (C4742-95), at 100 and 400 magnification after sedimentation for at least 24 h in Utermöhl chambers (Utermöhl, 1958). These samples were identified to the lowest genus or species level according to Scott and Marchant (2005) and Tomas (1997). The error sources of the Utermöhl method were corrected by the mean square estimate calculation with finite population corrections as described in

Sournia (1986) and Sun and Qian (2002). *Phaeocystis* colony abundances were determined immediately after sampling with 15 mL unpreserved samples under a dissecting microscope.

Samples (400–1000 mL) for taxon-specific pigments were filtered onto GF/F filters (Whatman) under low vacuum and frozen immediately in liquid nitrogen for later analysis using high performance liquid chromatography (HPLC). The pigments were separated on an automated Hewlett Packard 1050 HPLC system using a reverse-phase Waters Symmetry C-8 column and a solvent gradient containing methanol, aqueous pyridine, acetone, and acetonitrile (Zapata et al., 2000; DiTullio and Geesey, 2002). A diode array detector recorded pigment spectra over the wavelengths 350–600 nm and continuous chromatograms at 410, 440, and 455 nm every 5 s. Chl-*a* and *c* were also quantified using an HP 1046A fluorescence detector with excitation of 421 nm and emission at 666 nm (optimized for Chl-*a*). Injections of pigment standards isolated from a variety of unialgal cultures maintained in the laboratory were used to calibrate the system (DiTullio and Geesey, 2002).

2.4. Dissolved nutrients and iron

Dissolved macronutrient samples were taken using clean syringes directly from the incubation bottles. Samples were immediately 0.2 μm filtered and analyzed at sea using a Lachat Quickchem FIA+ series 8000 with an autoanalyzer method modified from WOCE protocols (Gordon et al., 1993). The nutrient measurements had a precision of approximately 1% based on replicate analysis.

Samples for total dissolved iron were filtered through 0.4 μm track-etched polycarbonate filters (Nuclepore Whatman) and acidified to pH 1.7 with 4 mL^{-1} Q-HCl (cleaned by sub-boiling quartz distillation) then measured using adsorptive cathodic stripping voltammetry (ACSV) (Buck et al., 2007). The voltammetric system was a Princeton Applied Research (PAR) 303A interfaced with a computer-controlled AutolabII potentiostat/galvanostat (Eco Chemie). The working electrode was a "large" mercury drop (2.8 mm^2), the reference electrode was Ag/saturated AgCl, saturated KCl, and the counterelectrode was a platinum wire. Reagents were prepared as follows: A 5 mmol L^{-1} salicylaldoxime (SA: Aldrich, ≥98%) solution was prepared in Q-MeOH and stored in the refrigerator. A final concentration of 25 μmol L^{-1} SA was used for total dissolved iron measurements. A 1.5 mol L^{-1} borate buffer was prepared as previously described (Lohan et al., 2002). Iron standards were prepared from dilution of a 1000 ppm atomic absorption standard with pH 1.7 Q-HCl. Acidified samples were microwaved twice for 15 s at 1100 W to release dissolved iron from organic ligands (Bruland et al., 2005), neutralized immediately with cool 1 mol L^{-1} Q-NH_4OH, and buffered to pH 8.2 with borate buffer. Iron and SA additions were then made, and after ACSV analysis, iron concentrations were determined from a linear regression of the standard addition curve. The detection limit was 0.02 nmol L^{-1}, calculated from three times the standard deviation of a 0.05 nmol L^{-1} iron addition. Sample analytical deposition times were 60–400 s. Total dissolved iron concentrations were measured at the initial and final timepoints; due to volume limitations, the three replicates for each treatment were combined, and values and errors presented are the means and analytical variability from triplicate analyses on the combined sample for each treatment.

2.5. Particulate matter

POC and PON samples (100–200 mL) were collected by filtration onto pre-combusted (450 °C, 2 h) Whatman GF/F glass fiber filters, which were then analyzed using a Carlo Erba NA1500 elemental analyzer/Conflo II device and a Finnigan Delta Plus mass spectrometer at the Stanford University Stable Isotope Biogeochemistry Laboratory. Elemental compositions were measured using the mass 44 beam intensity (V) on the Delta Plus, calibrated against the mass 44 beam intensity of at least five certified reference standards that were analyzed throughout the course of each run of 40 unknowns. Relative reproducibility of the acetanilide standard averaged 0.11% for N and 0.65% for C.

Samples (100–200 mL) for particulate organic phosphate (POP) were filtered onto pre-combusted Whatman GF/F glass fiber filters, and rinsed with 2 mL of 0.17 mol L^{-1} Na_2SO_4. The filters were then put into 20 mL pre-combusted (450 °C) borosilicate vials with 2 mL of 0.017 mol L^{-1} $MgSO_4$, dried at 95 °C, and stored in a dessicator. Prior to analysis, vials were combusted at 450 °C for 2 h; then 5 mL of 0.2 mol L^{-1} HCl was added into each vial after cooling. Vials were tightly capped and heated at 80 °C for 30 min. The standard molybdate colorimetric method (Solozano and Sharp, 1980) was used to analyze the digested POP samples. For biogenic silica (BSi) analysis, 100–200 mL samples were filtered onto 0.6 μm 47 mm polycarbonate filters, dried at 60 °C, and stored at room temperature until analysis. The samples were analyzed following the method of Brzezinski and Nelson (1995).

2.6. Photosynthesis versus irradiance curves (P–E curves)

P–E curves were determined using ^{14}C-uptake measurements in a small-volume photosynthetron (van Hilst and Smith, 2002). Irradiance levels in the on-deck incubators were within the range used in the *P/E* experiments (0–325 μE m^{-2} s^{-1}). Samples (65 mL) collected from each experimental treatment were mixed with ca. 150 μCi $NaH^{14}CO_3$ (pH=9.6), from which 2 mL samples were placed in each of 32 glass scintillation vials; the samples were then incubated under a range of irradiances from 0 to 600 μmol photons m^{-2} s^{-1}. The irradiance was measured once per day. The incubation temperature was regulated by a high-volume water bath with recirculating coolant to maintain the temperature close to that in the Ecostat continuous incubation systems (~0 °C). After 2-h of incubation, 0.5 mL of 1.0 N HCl was added to the vials to terminate photosynthesis. The samples were then vented in a hood for at least 24 h to remove inorganic ^{14}C. Then, 5 mL Ecolume® scintillation fluor was added, after which samples were kept in the dark for another 24 h to reduce chemiluminescence, and counted on a Packard liquid scintillation counter. Total inorganic ^{14}C-bicarbonate availability was measured by counting a 0.1-mL aliquot (to which 0.05 mL β-phenethylamine, a CO_2 trap, was added) directly in Ecolume. The *P–E* curves were fit to the Webb et al. (1974) empirical model

$$P^B = P^B_m[1-e^{-\alpha E/P^B_m}] \quad (1)$$

in which P^B=the rate of photosynthesis normalized to chlorophyll *a* [mg C (mg chl-*a*)$^{-1}$ h^{-1}], $P_m{}^B$=the maximum rate of photosynthesis in the absence of photoinhibition, α=the initial, light-limited, photosynthetic rate [mg C (mg chl-*a*)$^{-1}$ h^{-1} (μmol photons m^{-2} s^{-1})], and *E*=irradiance (μmol photons m^{-2} s^{-1}). The data were fit to this equation using SigmaPlot (version 10). In parallel, the data were fit to the model of Platt and Harrison (1980) to assess photoinhibition; however, significant photoinhibitory effects were noted in less than 10% of the measurements, and were therefore ignored in all.

The parameter values resulting from the non-linear regressions were compared using the non-parametric Kruskal–Wallis analysis of variance (ANOVA) and a posteriori Mann–Whitney

tests, as the data did not meet the normality and variance assumptions of the ANOVA. A critical p value of 0.05 was selected a priori for evaluation of all parameters. Systat (version 12) was used to perform the statistical analyses.

2.7. Photochemical efficiency of PSII

Measurements of photochemical efficiency of PSII were made with a MBARI bench-top fast repetition rate fluorometer (FRRF) (Kolber et al., 1994). Water samples for measurements were collected, immediately placed on ice, and kept under low light (5–10 μmol photons m^{-2} s^{-1}) for approximately 30–40 min. Minimal (F_0) and maximal (F_m) fluorescence were calculated from each single turnover (ST) saturation curve. The maximum quantum yield efficiency for PSII (F_v/F_m) was calculated (Genty et al., 1989) by normalizing F_m by the difference between the fluorescence at saturation (F_m) and the minimum fluorescence (F_0):

$$\Phi_{PSII}^{max} = \frac{F_m - F_0}{F_m} = \frac{F_v}{F_m} \quad (2)$$

To avoid condensation on the exterior of the cuvette due to the temperature difference between the cold seawater and the laboratory air, the light and cuvette chamber where constantly flushed with dry nitrogen gas.

2.8. Statistics

Interactive effects of light, temperature, and CO_2 were statistically analyzed for final day data using the freeware statistical software program R version 2.5 (http://www.r-project.org). A modified three-way ANOVA test was used to detect two- and three-way interactions among the variables. This test is based on Algina and Olejnik (1984), as described and implemented by Wilcox (1997). It uses 20% trimmed means as a measure of location and a percentile t bootstrap method to test for significance. This modified test was chosen over the standard three-way ANOVA because it does not have the standard assumptions of normality or homoscedasticity and generally has higher power. All testing was done at the α=0.05 level. A similar modification of the standard two-way ANOVA was used to determine the effects of light and iron on *Phaeocystis* colony formation since CO_2 treatment replicates were combined to obtain enough sample volume for analysis (Wilcox, 2003). Prior to testing the significance of the nutrient ratios, outliers were identified and removed using the Hampel identifier, as modified by Rousseeuw and van Zomeren (1990). Pair-wise tests (except for photosynthetic parameters) were conducted with one-way ANOVA (Kinnaer and Gray, 1997).

3. Results

3.1. Carbonate system measurements

The carbonate system was stable during the course of the incubation, and pCO_2 was maintained very close to the targeted values of ~380 ppm for low CO_2 treatments and ~750 ppm for high CO_2 treatments. pCO_2 values calculated from DIC and pH values on the final sampling day are shown in Table 1.

3.2. Photosynthetically active radiation (PAR)

Due to weather-related variability, the mean daily light levels in the high-light incubator varied from 52 to 276 μmol photons m^2 s^{-1}, and from 11 to 58 μmol photons m^2 s^{-1} in the low-light incubator (Fig. 1). The magnitude of the error bars associated with the daily mean PAR values reflects both the diurnal light cycle, and short-term variations induced by clouds. Over the first 12 days of the experiment initially sunny weather was replaced with gradually increasing cloud cover, followed by 5 days of bright sunshine, and then heavy overcast again over the final 24 h.

3.3. Phytoplankton biomass and nutrient concentrations

Chl-*a* concentrations responded significantly to different irradiances and iron concentrations (Fig. 2a and b). In all pCO_2 and iron treatments, the average total Chl-*a* concentration during the course of the incubation was significantly lower (50%) in the high-light treatments compared with the low-light ones. At both irradiance levels, Chl-*a* was significantly increased by iron enrichment, with almost doubled concentrations on T18 in the iron-enriched treatments compared with the controls ($p < 0.05$). The initial Chl-*a* concentration (T0) was 6.9 ± 0.2 μg L^{-1}. After the first 5 days of batch incubation, total Chl-*a* concentration greatly increased in the four treatments under low light (the highest value was close to 20 μg L^{-1} on T5). This increase over the first 5 days was, however, modest (~1–2 μg L^{-1}) in the high-light treatments.

After the continuous incubation started on T5, Chl-*a* showed an initial drop as a result of dilution. From T10, Chl-*a* concentrations were relatively stable in most of the iron-enriched treatments until the end of the experiment (Fig. 2a and b). In the low iron treatments Chl-*a* concentrations continued to slowly decline throughout the experiment, mostly likely due to the iron-limited assemblage growth rate being less than the 0.4 d^{-1} dilution rate. This decline was especially evident in the low-light, control bottles (Fig. 2). Different CO_2 concentrations did not have significant effects on Chl-*a* concentrations.

On the final sampling day, the measured Chl-*a* concentrations in all treatments were higher by about 2 μg L^{-1} than the previous day's values at T17. This possibly was due to the different

Table 1
The seawater carbonate buffer system and total dissolved iron concentrations in the eight treatments on the final sampling day (T18).

Treatments	DIC concentration (μmol kg^{-1})	pH	Calculated pCO_2 (ppm)	Total dissolved iron (nM)
Low light, control, low CO_2	2181.7	8.13	381	0.19 (0.02)
Low light, control, high CO_2	2251.6	7.84	776	0.29 (0.008)
Low light, Fe, low CO_2	2164.9	8.12	385	0.98 (0.004)
Low light, Fe, high CO_2	2220.7	7.86	731	0.83 (0.006)
High light, control, low CO_2	2166.9	8.13	374	0.13 (0.02)
High light, control, high CO_2	2209.2	7.86	736	0.09 (0.01)
High light, Fe, low CO_2	2131.8	8.14	363	0.34 (0.008)
High light, Fe, high CO_2	2222.6	7.85	749	0.45 (0.007)

Total dissolved iron values presented are the means, and errors are the analytical variability from triplicate analyses of one sample combining all three replicates in each treatment.

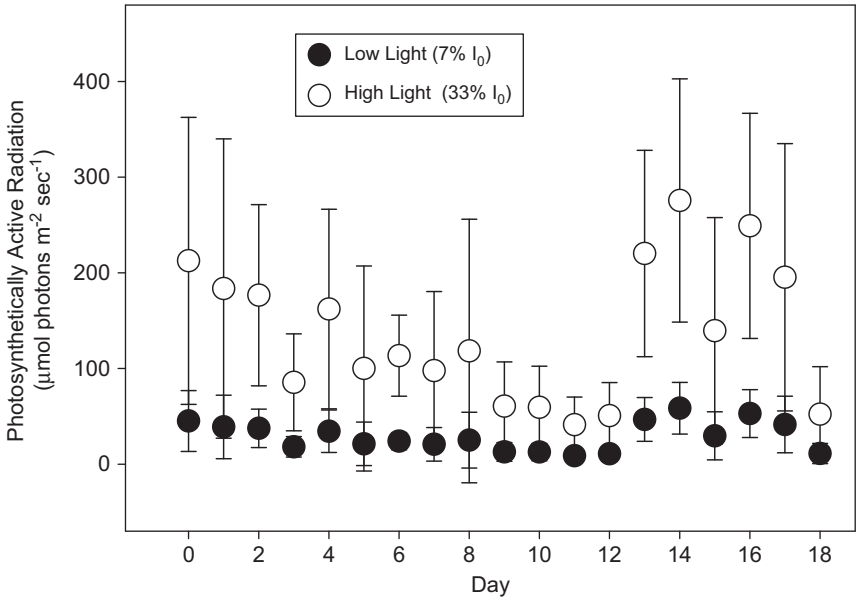

Fig. 1. Photosynthetically active radiation (PAR, μmol photons m^2 s^{-1}) in the two light treatments during the entire course of the 18 day experiment. Symbols represent the daily means and error bars are the standard deviations of continuous measurements; shown are photon flux densities for treatments in the high-light incubator (33% of incident PAR, open circles) and the low-light incubator (7% of incident PAR, closed circles).

sampling strategy used at the final timepoint. Instead of syringe sampling on T18, samples were taken directly from the bottles after vigorous shaking, potentially dislodging any algal cells growing on the walls of the bottles. It is also possible that this final day increase in Chl-*a* reflected photoadaptation to the low incident irradiance experienced over the previous 24 h (Fig. 1).

POC concentrations also responded significantly to the iron enrichment under high light, but iron effects were less obvious under low light (Fig. 2c and d). The initial POC concentration was 36.2 ± 2.2 μM and after 5 days of batch incubation the values were greatly increased, with higher concentrations found in the iron-addition treatments, similar to the trend of Chl-*a* concentrations. After the dilution started, POC concentrations declined slowly at low light in all four CO_2 and iron treatments for 6 days. POC concentrations then were constant with slightly higher values in the iron-enriched treatments for the next 5 days, suggesting that biomass accumulation was largely in balance with the availability of the limiting nutrient in the dilution water. The final POC values were slightly lower, perhaps due to the way this timepoint was sampled, or to increased light limitation during the last day (see below).

Under high light in the iron-enriched treatments, POC values were higher and relatively steady throughout the dilution portion. The high-light control treatments showed slow initial declines, followed by a period of relatively balanced concentrations and a final day drop, just as all treatments did under low light. The PON concentrations showed trends that were similar in nearly every way with those of POC under both high light and low light, and with regard to changing iron availability as well (Fig. 2e and f). Changing CO_2 had no apparent effect on either POC or PON concentrations in any treatment (Fig. 2c–f).

The trends in POC and PON concentrations in both of the low-light treatments and in the high-light, control treatment roughly parallel the mean daily PAR changes. The initial declines in particulate concentrations in these three treatments are similar to the declines in ambient irradiance until about day 12 (Fig. 1). The period of stable, sunny weather until day 17 is reflected in relatively constant levels of POC and PON over this period, and the resumption of heavy overcast on the final day is mirrored by the lower levels of particulates in the final sample (Fig. 2a–f).

Under both irradiances, there was a decline in POC and PON from T17 to the final day (T18). As discussed above, this may have been a net growth response to the reduced light levels experienced over the final 24 h of the experiment (Fig. 1), or could have been caused by the different sampling technique used on the last day. The T18 samples were taken directly from the sampling bottles, but before that, all the POC samples were taken from the outflow bottles. Although the outflow bottles were kept chilled and in the dark, the samples could have grown marginally in "batch" mode over the 24 h between collections.

Chl-*a*:POC ratios (Fig. 2g and h) were somewhat higher at every timepoint after T0 in the low-light treatments compared to the high-light treatments; iron and CO_2 availability did not significantly affect the ratios ($p > 0.05$) on most sampling days. The large increase in Chl-*a*:POC in all low-light treatments on the last day is due to both increased Chl-*a* (Fig. 2a) and reduced POC (Fig. 2c) concentrations, supporting the suggestion of a response to the very overcast conditions experienced over the final 24 h (Fig. 1).

The nutrient concentrations during the incubation also responded to different experimental treatments, especially those with different iron concentrations. Nitrate, phosphate, and silicic acid concentrations all dropped significantly during the first 5 days of batch incubation, but were much more stable over the course of the continuous incubation. None of the macronutrients were depleted in any of the treatments throughout the incubation (Fig. 3), supporting the suggestion that no macronutrient was limiting in the continuous culture system. At both irradiance levels, all the nutrient concentrations were significantly lower in the iron-enriched treatments than the controls from T4 to T18, especially in the last few days of the experiment. Neither nitrate nor phosphate concentrations showed significant differences between different irradiances (Fig. 3a and b); however, when other experimental conditions (iron concentration and pCO_2) were the same, silicic acid concentrations were slightly and significantly lower ($p < 0.05$) in the low-light treatments, and this trend was consistent on each day from T4 to T18 (Fig. 3c). As with Chl-*a*, POC, and PON, nutrient concentrations were not influenced by different CO_2 concentrations.

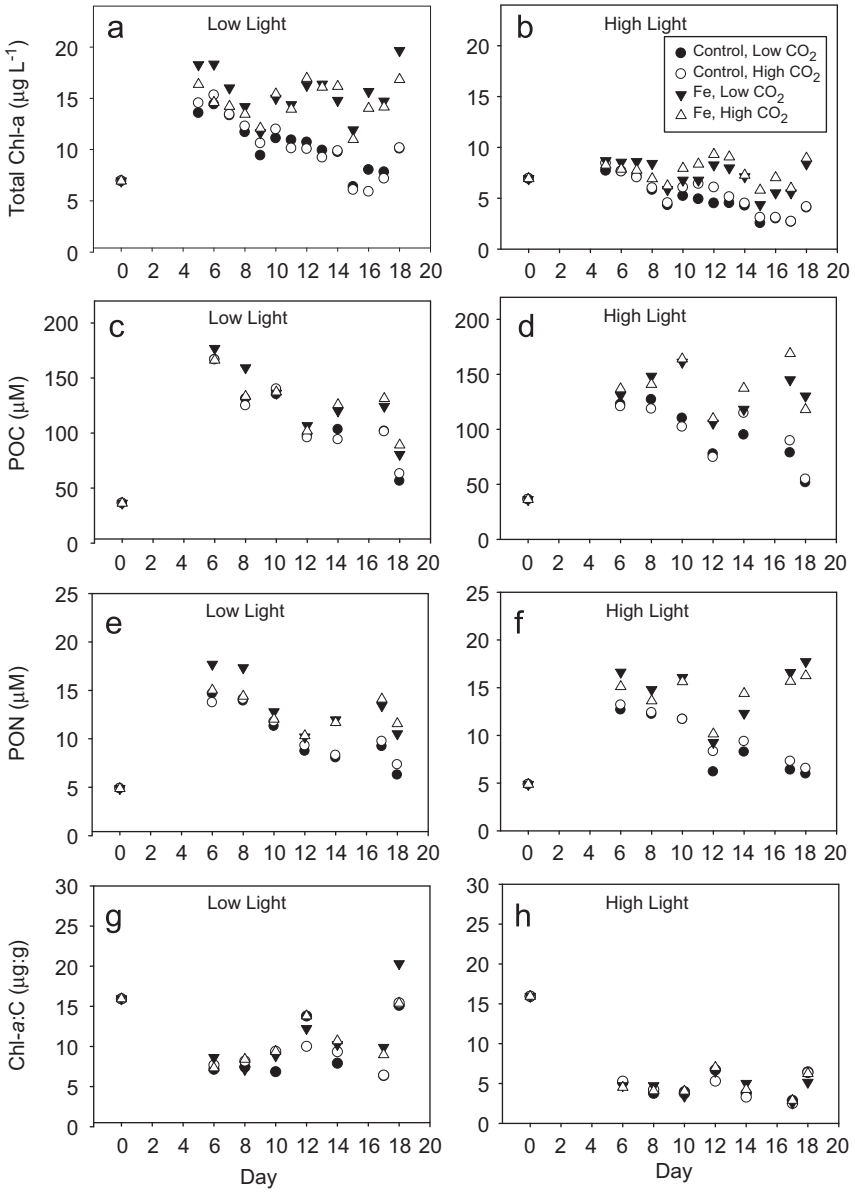

Fig. 2. Phytoplankton biomass of the eight experimental treatments during the time course of the incubation. (a) Total Chl-*a* ($>0.2\,\mu m$, $\mu g\,L^{-1}$) concentrations at low light; (b) total Chl-*a* ($>0.2\,\mu m$) concentrations at high light; (c) POC concentrations (μM) at low light; (d) POC concentrations (μM) at high light; (e) PON concentrations (μM) at low light; (f) PON concentrations (μM) at high light; (g) Chl:C ratios (μg:g) at low light; and (h) Chl:C ratios (μg:g) at high light. (Error bars not shown for clarity.)

Total dissolved iron was measured in the filtered seawater medium carboy reservoirs supplying the experimental bottles directly after water collections and iron additions, and again at the end of the experiment. Initial and final dissolved iron concentrations were 0.18 ± 0.01 and 0.15 ± 0.01 nM in the control carboy, and 1.08 ± 0.01 and 1.04 ± 0.01 nM in the iron-enriched carboy, respectively (Table 1). Dissolved iron levels were lower at high light than at low light in both controls and iron treatments; no clear trends in iron concentrations were evident between high and low CO_2 treatments.

3.4. Phytoplankton taxonomic composition

Photosynthetic pigment analyses indicated that there were two main phytoplankton groups in the incubations when the experiment started: diatoms (fucoxanthin, (Fuco); 965 ± 38 ng L^{-1}) and haptophytes, specifically *P. antarctica* (19′-hexanoloyxyfucoxanthin, (Hex) $439 \pm 21\,ng\,L^{-1}$). Changes in Fuco and Hex indicated that the relative dominance of the two algal groups was greatly affected by irradiance and iron addition. Pigment samples suggested that the initial community was dominated by diatoms (Fuco:Hex > 2), and this result was confirmed by microscopy. Fuco concentrations were significantly ($p < 0.05$) lower under high light than low light in all the iron/pCO_2 treatments (Fig. 4a). At both irradiances Fuco concentrations significantly increased in the two iron-enriched treatments ($p < 0.05$, except for the high-light, low CO_2 treatment which showed large variability between replicates), indicating higher diatom abundance after iron enrichment. Under low light, higher Hex values ($p < 0.05$) were found in the two low CO_2 treatments at equivalent iron concentrations (Fig. 4b).

The ratios of Fuco:Hex on the final sampling day changed in response to the different irradiances and iron concentrations (Fig. 4c). Under both irradiances, higher ratios were found in the two iron-enriched treatments ($p < 0.05$) relative to the control,

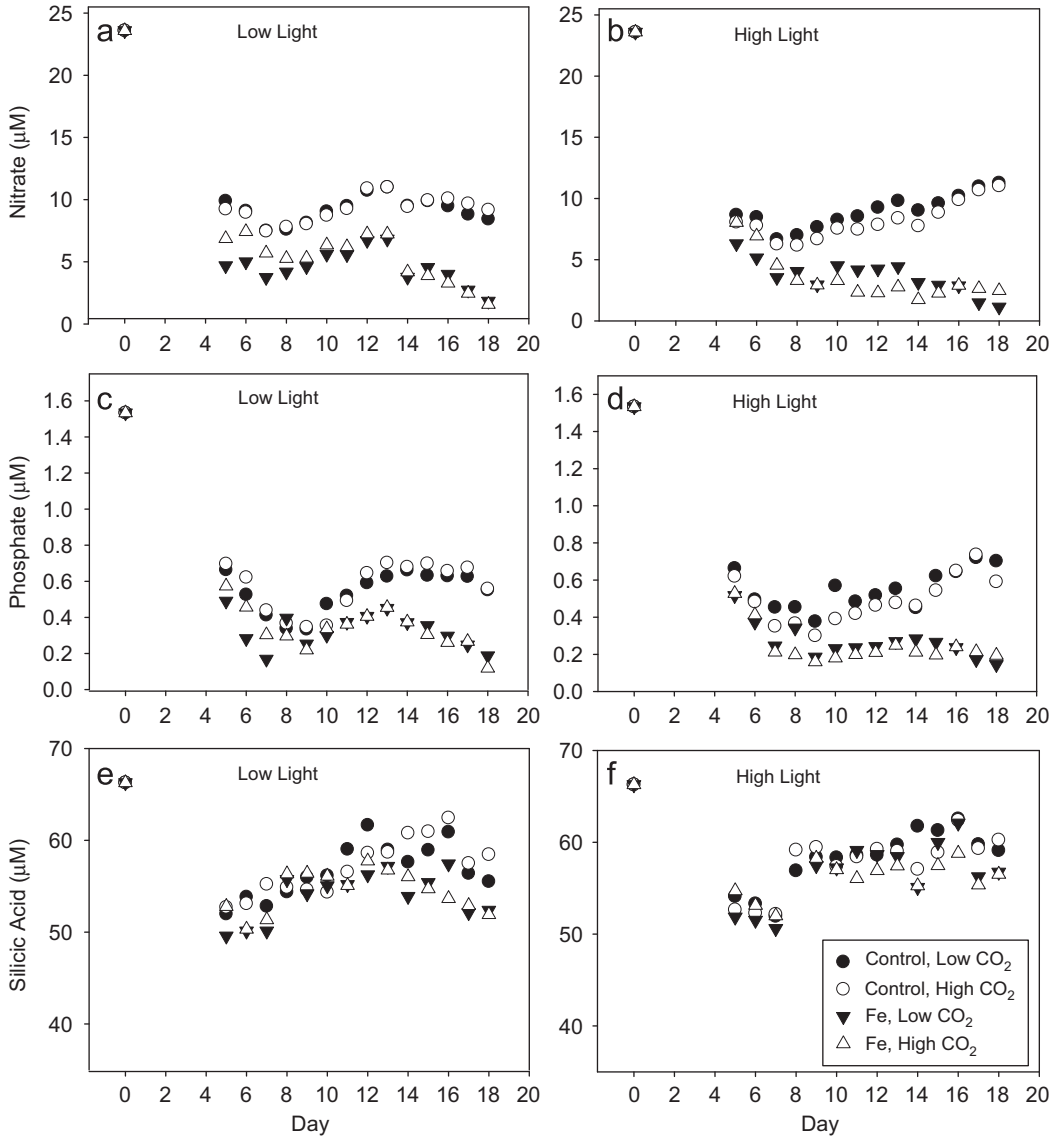

Fig. 3. Dissolved nutrient concentrations (μM) of the eight experimental treatments during the time course of the incubation. (a) Nitrate at low light; (b) nitrate at high light; (c) phosphate at low light; (d) phosphate at high light; (e) silicic acid at low light; and (f) silicic acid at high light. (Error bars not shown for clarity.)

indicating that diatoms were more responsive to iron enrichment than *Phaeocystis*. In addition to taxonomic changes, photoadaptation in the bottles could have influenced the levels of algal accessory pigments, but both Fuco and Hex should have been affected by this process. This suggests that despite photoadaptive changes, Fuco:Hex ratios still should offer a meaningful indication of community composition changes. Different CO_2 concentrations did not have significant effects on either the concentrations of the two pigments or their ratios.

The ratio of centric to pennate diatoms abundance was significantly influenced by CO_2 and iron enrichment (Fig. 5). Throughout the experiment, the two main diatoms present in the incubation were the centric species *Chaetoceros lineola* and the pennate species *Cylindrotheca closterium*. The cell abundance ratio of *Chaetoceros*:*Cylindrotheca* in the initial community was 0.21, and on T18 the ratios had decreased in all the low-light treatments. All of the low-light ratios were significantly higher under high pCO_2 on the final day ($p<0.05$, Fig. 5). Under high light, the centric:pennate ratios in the control, high CO_2 and iron, high CO_2 treatments were much higher than in the other two treatments, with averaged values of 0.47 and 0.26, respectively. In general, the dominance of the large centric *Chaetoceros* relative to the smaller pennate *Cylindrotheca* was enhanced under high CO_2 regardless of other factors, but especially under high light.

P. antarctica colony abundance was significantly affected by increased irradiance and iron enrichment, but not by CO_2 (Fig. 6). High and low pCO_2 treatments were combined during colony enumeration to increase the power of the statistical tests, because there were no differences between pCO_2 treatments. On the final sampling day, colony abundance at low light was lowest in both the control and +iron treatments (<1 colony mL^{-1}). Colony abundance was significantly ($p<0.05$) increased by high light alone (with no Fe addition), but by far the greatest colony abundance ($6\,mL^{-1}$) was observed in the high-light, high-iron treatment (Fig. 6). The much higher concentration of colonies in this treatment was evident immediately from visual inspection of the bottles on the final day, especially compared to both low-light treatments. The sizes of the colonies were not significantly different between treatments.

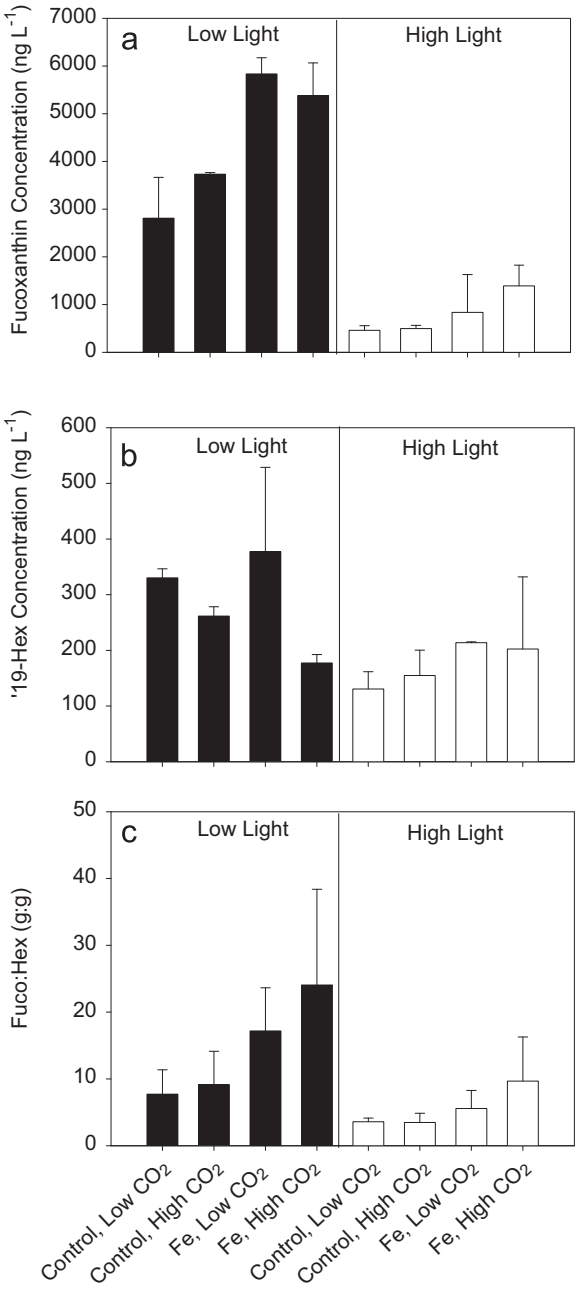

Fig. 4. Major phytoplankton accessory pigments concentrations in the eight treatments on the final sampling day (T18). (a) Fucoxanthin concentrations (ng L^{-1}); (b) '19-Hex concentrations (ng L^{-1}); (c) ratios of fucoxanthin concentration to '19-Hex concentration (g:g).

3.5. Elemental ratios

The biogenic silica (BSi) concentration was greatly affected by iron concentrations (Fig. 7a), in parallel with the Fuco:Hex ratio and diatom abundance. Under both low light and high light, the average BSi concentrations in the iron-enriched treatments were almost 1.5-fold higher than in the controls. Irradiance and pCO_2 did not significantly affect BSi concentrations. After normalization to POC concentrations, however, the BSi:POC ratios showed significantly different patterns under different irradiance levels (Fig. 7b). At low light, the ratios were not significantly different among the four Fe/pCO_2 treatments, with an average value of 0.16; but at high light, the ratios in the two iron-enriched treatments (averaged value 0.10) were significantly lower than in the two controls (average value 0.15). The BSi:PON ratios had trends that were similar to those of BSi:POC ratios (Fig. 7c).

Particulate C:N:P elemental ratios were also influenced by irradiance and/or different iron concentrations (Fig. 8). For POC:PON ratios, the only significant differences were under high light, where control treatments had slightly higher values in the iron-enriched treatments (Fig. 8a). Both the POC:POP (Fig. 8b) and PON:POP (Fig. 8c) ratios were significantly higher ($p<0.05$) at high light than low light. This light-related trend in elemental stoichiometry was opposite to the trend in the Fuco:Hex ratios, once again suggesting higher relative *Phaeocystis* abundance at high light since this prymnesiophyte has characteristically higher C:P and N:P ratios than diatoms (Arrigo et al. 1999).

3.6. Photosynthetic parameters

The photosynthetic parameters were mainly affected by irradiance and iron. For the P^B_{max} values, there was a substantial increase from the T0 sample in all treatments during the experiment, suggesting acclimation to the ambient irradiance field. Under low light, the P^B_{max} values in the iron-enriched treatments were greater at the end of the experiment, but this trend could not be tested statistically due to volume limitation and missing samples, as only a single replicate was available for analysis in the high Fe treatments (Table 2). A similar, more pronounced trend ($p<0.05$) was observed under high light, where the greatest P^B_{max} values were observed under high light with added iron on the final sampling day. Increases in α through time were observed under both light levels, suggesting an acclimation to higher than *in situ* irradiance levels. The increases were larger in the high-light treatments, but the high variance of the data made the trend statistically insignificant. Highest α values occurred with both irradiances under the iron-enriched and high pCO_2 treatments on T18 (Table 2). CO_2 did not seem to influence the photosynthetic parameters or responses. Some of the light-related trends in Chl-*a*-normalized *P–E* parameters may have been influenced by the somewhat higher Chl-*a*:POC ratios in the low-light treatments (Fig. 2g and h), but the lack of significant iron-related changes in Chl-*a*:POC suggests that the trends in P^B_{max} and α driven by iron availability were not caused by normalization to Chl-*a*.

Quantum yields were initially low (0.30; Table 2) and the cultures quickly recovered, achieving an F_v/F_m close to 0.60 on Day 6, and then having reduced quantum yields thereafter. Light had a significant effect on F_v/F_m ($p<0.05$), with high-light conditions exhibiting a reduced quantum yield (on average 0.443) when compared to those found in the low-light environment (mean=0.509). Although F_v/F_m values were usually slightly higher in the iron-enriched bottles than in the controls at the same irradiance and pCO_2, in general light, rather than iron or CO_2, appeared to be the major factor influencing photosynthetic efficiency.

3.7. Interactive effects

The three-way ANOVA tests results (Table 3) suggested that iron and light had significant interactive effects on the final day POC and PON concentrations, BSi:POC, BSi:PON, Fuco concentrations, *Phaeocystis* colony abundance, and centric versus pennate diatom abundances. The final centric to pennate diatom ratio was the only parameter that showed significant two-way interactive effects of light and CO_2 and iron and CO_2, as well as a significant three-way interaction between CO_2, iron and light (Table 3).

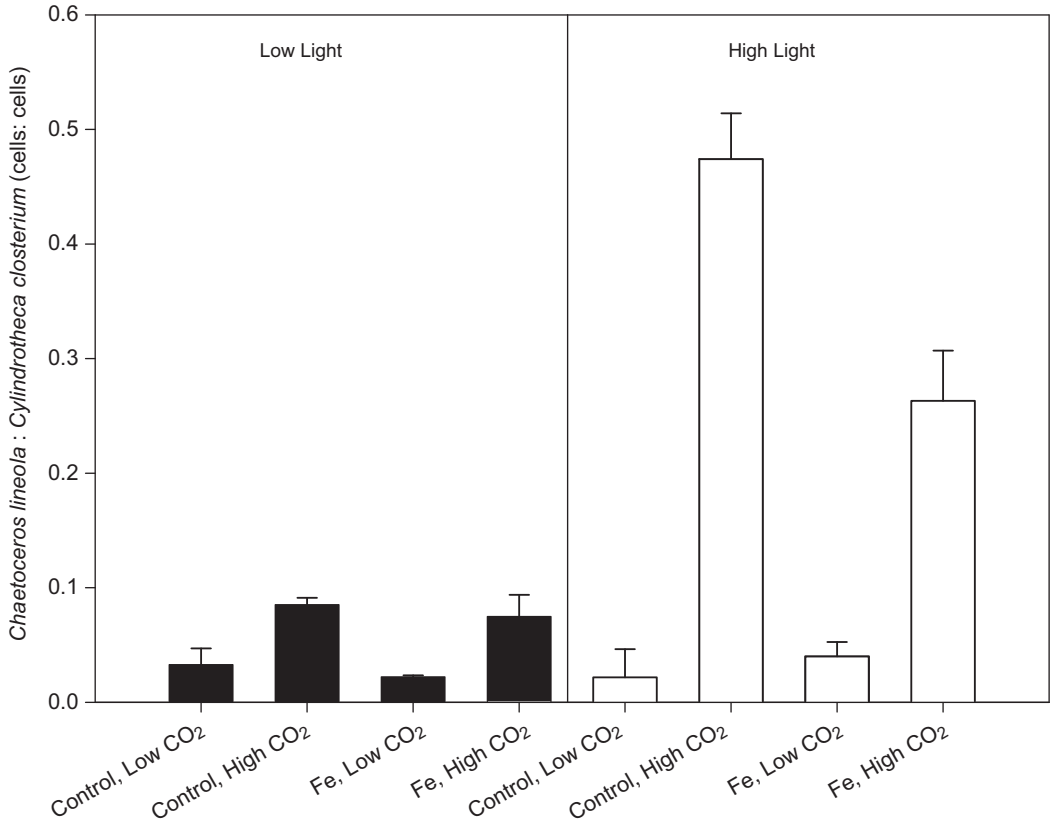

Fig. 5. Ratios of cell abundance of the two major diatom species (*Chaetoceros lineola*:*Cylindrotheca closterium*, cells:cells) on the final sampling day (T18). Error bars represent standard deviations (n=3).

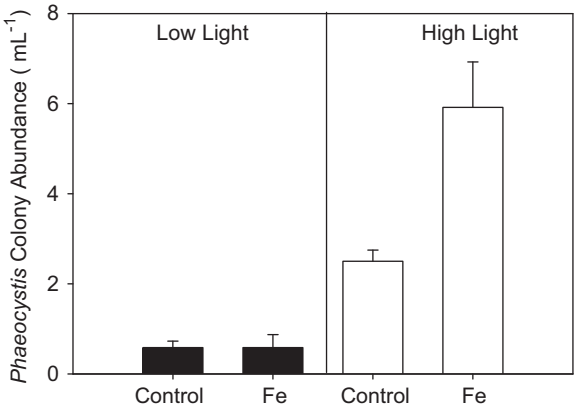

Fig. 6. *Phaeocystis antarctica* colony abundance (mL^{-1}) on the final sampling day (T18). Error bars represent standard deviations (n=6, high CO_2 and low CO_2 treatments were combined during sample analysis).

4. Discussion

The results of this continuous culture experiment indicated that Ross Sea phytoplankton structure and biogeochemistry respond strongly to changing irradiance and iron, and to a much lesser degree to increased CO_2. High irradiance significantly increased the relative abundance of *P. antarctica* relative to diatoms, and the absolute abundance of *P. antarctica* colonies. Iron enrichment greatly increased overall phytoplankton biomass, diatom relative abundance, *P. antarctica* colony abundance under high light, dissolved nutrient drawdown, and some photosynthetic parameters (P^B_{max}, α, and quantum yields). CO_2 concentration mainly affected the relative abundance of the dominant diatom species, with high pCO_2 favoring the large, chain-forming, centric diatom *C. lineola* over the smaller, solitary, pennate diatom *C. closterium*.

Some aspects of this natural community continuous culture experiment closely resemble classical laboratory chemostat dynamics (Veldkamp, 1976). For instance, the relatively constant biomass achieved in the high-iron, high-light treatment (Fig. 2) suggests that biomass was a function of the concentration of the limiting nutrient iron in these bottles, and that algal growth rates were in balance with the dilution rates of the system. Although it is a continuous culture system, the natural community system nevertheless does not fully meet the requirements of a true chemostat. There are several key conditions that are not met using this shipboard Ecostat system or similar systems, as has been discussed previously (Hutchins et al., 2003, Hare et al., 2005, 2007a, b; Feng et al., 2009, Pickell et al., 2009). Unlike a true chemostat in which irradiance is held constant, our deckboard system experiences variable light levels with diurnal cycles and short-term changes due to weather. Another difference is the fact that net phytoplankton growth rates (which incorporate any grazing or viral lysis mortality occurring in these mixed natural communities) must balance dilution rates, not intrinsic growth rates as in a laboratory chemostat. Our Ecostat examines the weighted average responses of many species each with its own individual half-saturation constants for light, iron, nutrients, temperature, etc., and not the physiological response of a single species, as does a lab chemostat.

The most important reason that this experiment cannot be fully considered in classical chemostat terms, however, is because of its multi-variate nature. Each treatment was designed to be limited by a different combination of controlling factors, including

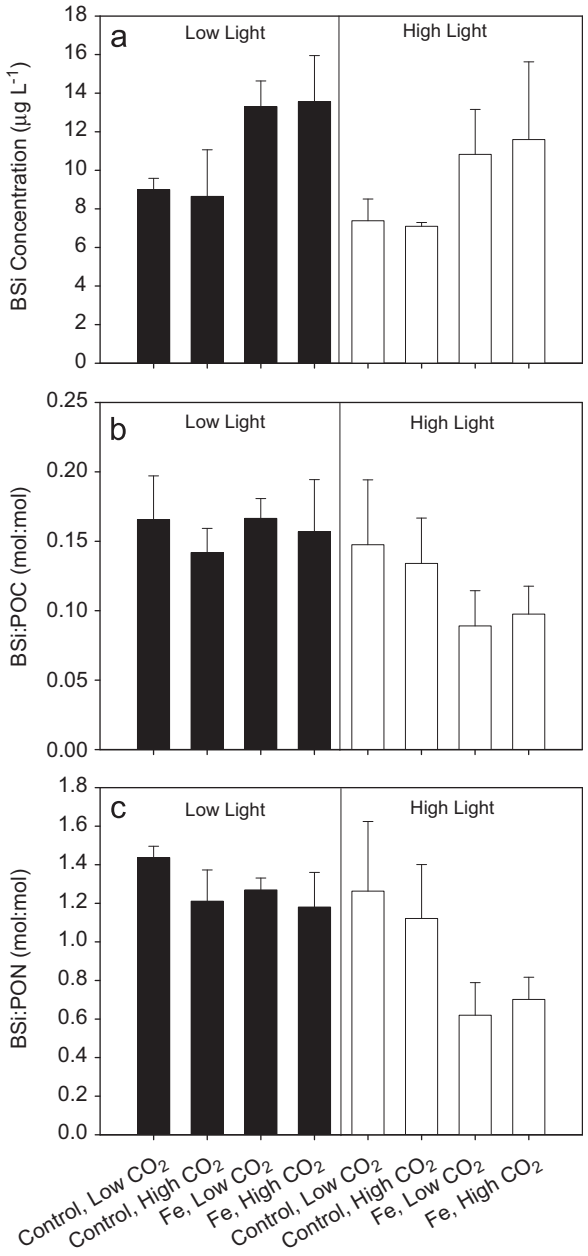

Fig. 7. (a) BSi concentrations (μM) of the eight treatments on the final sampling day (T18); (b) ratios of BSi:POC concentrations (mol:mol) of the eight treatments on the final sampling day (T18); and (c) ratios of BSi:PON concentrations (mol:mol) on the final sampling day (T18). Error bars represent standard deviations (n=3).

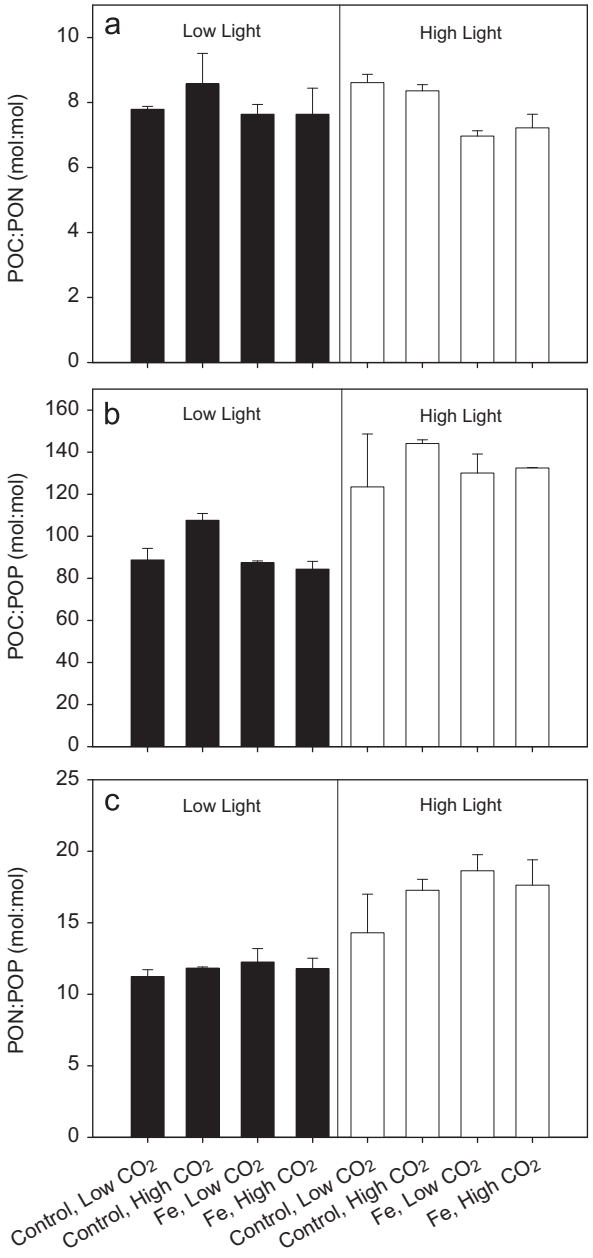

Fig. 8. Elemental ratios (mol:mol) of the eight treatments on the final sampling day (T18). (a) POC:PON ratios; (b) POC:POP ratios; and (c) PON:POP ratios. Error bars represent standard deviations (n=3).

iron limitation (high-light, control), light limitation (low-light, iron-enriched), iron-light co-limitation (low-light, control), or iron and light replete (high-light, iron-enriched). CO_2 effects were less evident, except in the case of CO_2 control of diatom community structure. The iron-enriched bottles were unlikely to have been limited by the supply of this micronutrient, judging by the relatively high unused dissolved iron concentrations on the final day (0.34–0.98 nM) compared to those in the control bottles (0.09–0.29 nM, Table 1). Light limitation in particular would prevent algal growth rates from being dependent only on dilution rates, and biomass accumulation from being a simple function of the limiting nutrient concentration.

Our iron and light co-limitation results in particular have important implications for understanding controls on phytoplankton growth in many regions of the world ocean (Sunda and Huntsman, 1997; Strzepek and Harrison, 2004; Hopkinson and Barbeau, 2008). The lowest levels of POC and PON during the latter part of our experiment were observed in the low-light, control treatment bottles (Fig. 2c and e). Chl-*a* in this treatment also declined steadily throughout the experiment (Fig. 2a), suggesting that net growth rates of these iron/light co-limited phytoplankton did not achieve a growth rate imposed by the dilution rate ($0.4\,d^{-1}$). These results emphasize the need to consider the interactive biological and biogeochemical influences of the very low iron concentrations and deep mixed layers that frequently characterize large parts of the Ross Sea, and the Southern Ocean in general.

Irradiance has been previously reported to be an important determinant of the distribution of diatoms and *P. antarctica* in the

Table 2
Photosynthetic parameters of the eight experimental treatments on the final sampling day (T18). Values in parentheses represent standard deviations (n=2 for P^B_{max} and α values; n=3 for FRRF measurements; except for values with "a").

Treatments	P^B_{max} (μg C (μg Chl-a)$^{-1}$ h^{-1})	α (μg C (μg Chl-a)$^{-1}$ (μmol m^{-2} s^{-1})$^{-1}$ h^{-1})	FRRF-based F_v/F_m measurement
T0	0.502[a]	0.013[a]	0.300[a]
Low light, control, low CO_2	2.369 (0.826)	0.037 (0.005)	0.481 (0.007)
Low light, control, high CO_2	1.965 (0.239)	0.085 (0.016)	0.526 (0.008)
Low light, Fe, low CO_2	2.914[a]	0.0388[a]	0.498 (0.008)
Low light, Fe, high CO_2	2.218[a]	0.0507[a]	0.529 (0.008)
High light, control, low CO_2	1.512 (0.396)	0.025 (0.003)	0.436 (0.008)
High light, control, high CO_2	1.294 (0.004)	0.043 (0.000)	0.433 (0.008)
High light, Fe, low CO_2	2.933 (0.770)	0.040 (0.003)	0.433 (0.008)
High light, Fe, high CO_2	3.549 (0.209)	0.073 (0.004)	0.469 (0.008)

[a] Due to sampling volume limitation and missing samples, only one sample was measured.

Table 3
Main effects and interactions among variables on the final day of the experiment. Asterisks represent significance at the α=0.05 level using a modified three-way ANOVA test on most parameters and two-way ANOVA on *Phaeocystis* colony abundance.

Parameter	Light	Fe	CO_2	Light+Fe	Light+CO_2	Fe+CO_2	Light+Fe+CO_2 three-way
POC concentration		***		***			
PON concentration	***	***		***			
POP concentration		***					
BSi concentration		***					
POC:PON		***					
POC:POP	***						
PON:POP	***						
BSi:POC	***			***			
BSi:PON	***	***		***			
Fucoxanthin concentration	***	***		***			
19-Hex	***						
19-Hex:Fuco	***						
Chl-*a*	***	***					
Phosphate		***					
Nitrate		***					
Silicic acid	***	***					
C:Chl-*a*	***						
Chaetoceros:*Cylindrotheca* (centric/pennate)	***	***	***	***	***	***	***
*Phaeocystis*colony abundance	***	***		***			

Ross Sea area. In general diatoms dominate in more stratified areas with shallower mixed layer depths (MLD), whereas *P. antarctica* mainly dominates in areas with deeper MLD (DiTullio and Smith, 1996; Arrigo et al., 2000; Smith and Asper, 2001). This has been suggested to be due to the relatively higher photosynthetic efficiency of the haptophyte at lower irradiance, compared to that of diatoms (Palmisano et al., 1986; Arrigo et al., 1999; Moisan and Mitchell, 1999).

However, in our incubation study we observed an opposite trend. Based on the pigment data the relative diatom abundance was lower at high light compared with low light, under comparable iron and CO_2 conditions. The ratio of diatoms to *P. antarctica* (as indicated by the Fuco:Hex ratio) suggested higher relative *P. antarctica* abundance at higher irradiance. Although laboratory cultures of *P. antarctica* have been shown to convert Hex to Fuco under iron-replete (μM levels) conditions (van Leeuwe and Stefels, 1998), experiments with more realistic iron concentrations observed in the Ross Sea (i.e. nM levels) revealed relatively low Fuco:Hex ratios (<0.15) under environmentally relevant iron-replete conditions (e.g. 2 nM; DiTullio et al., 2007). Consequently, Fuco:Hex ratios are still valid indicators of the relative abundance of diatoms versus *P. antarctica* in the Ross Sea. Smith and Asper (2001) also observed a similar trend in the Ross Sea, in that *P. antarctica* dominated in more stratified water with higher irradiances. They explained this anomaly as being possibly affected by a complex matrix of factors, including mixed layer depth and micronutrient concentrations. Similarly, van Hilst and Smith (2002) found no statistical difference in photosynthetic parameters between *P. antarctica* and diatoms. Our results suggest that if diatoms routinely outcompete *P. antarctica* in shallow, highly stratified mixed layers near melting ice in the Ross Sea, the reason may be due to factors other than just photobiology. Other potentially important biological or biogeochemical influences could include differential "seeding" of diatoms from ice algae stocks (Smith and Nelson, 1985), addition of ice-derived micronutrients, or differences in top–down control by grazers. Variations in the mechanisms driving stratification (i.e. salinity-driven stratification associated with melting ice versus temperature-driven stratification associated with wind relaxation events) could also have effects on the abundance of the two groups.

Our study found that under iron-amendment, *P. antarctica* cells were more likely to assume the colonial morphotype under higher irradiance than at low-light conditions. Colonial *P. antarctica* cells have been documented to be able to store a large proportion of photosynthetically fixed carbon extracellularly within the colony, mainly in the form of polysaccharides (Rousseau et al., 1994; Janse et al., 1996; Mathot et al., 2000; Robinson et al., 2003). These studies found that at higher irradiance, more photosynthate was generated and partitioned both into growth (cellular production) and mucous production by the colonial cells. This mucilageous carbon produced at higher irradiance has been hypothesized to be available for utilization by the cells for growth and metabolic processes over time (Lancelot and Mathot, 1985), and so could possibly facilitate survival if light becomes limiting

due to deep mixing events or ice formation. Divalent trace metals (e.g. Mn^{+2}) may also be luxuriously stored within the colonial matrix (Davidson and Marchant, 1987). Such carbon and micronutrient storage mechanism may offer colonial *P. antarctica* a potential competitive advantage over diatoms under some environmental conditions.

Arrigo et al. (1999) and Dunbar et al. (2003) reported a relative higher drawdown of CO_2 and nitrate per mole phosphate for *Phaeocystis* cells than diatoms. They pointed out the potential biogeochemical implications of this non-Redfieldian stoichiometric behavior for carbon export out of the mixed layer, although another study found that exported material in the Ross Sea conformed to Redfield stoichometry (Sweeney et al. 2000). We also observed increased elemental ratios of C:P and N:P in our experiments in which *P. antarctica* became dominant (Fig. 8), but only in treatments where irradiance was increased to 33% of the sea surface value. Thus, mixed layer depths and potential light limitation need to be considered when assessing the ability of *Phaeocystis* to export carbon more efficiently than diatoms (Arrigo et al., 1999; Dunbar et al., 2003).

Total biogenic silica production was enhanced in the high-iron treatments in which diatoms outcompeted *P. antarctica*. Despite this, community BSi:POC and BSi:PON ratios were higher in control treatments than in iron-amended bottles, an effect on diatom cellular silicification that has been observed in numerous iron-addition experiments in the past (Hutchins and Bruland 1998; Firme et al., 2003; Franck et al., 2003; Leblanc et al., 2005). These earlier studies did not examine irradiance effects, but in our experiment elevated BSi:POC and BSi:PON ratios in control bottles occurred only in our high-light treatments. Overall, our results suggest that light availability could play a key role in mediating the elemental ratio changes that characterize community dominance shifts between *P. antarctica* and diatoms in the Ross Sea.

Iron has been demonstrated to be perhaps the most critically limiting factor controlling phytoplankton growth in the high-nutrient low chlorophyll (HNLC) regions, including the Ross Sea (Martin et al., 1990b; Sedwick et al., 2000). In our study, the 1 nM continuous iron enrichment resulted in much higher phytoplankton biomass and higher nutrient drawdown both under high and low irradiance, consistent with the results of previous shipboard iron-addition experiments (Martin et al., 1990b; de Baar et al., 1990; Scharek et al., 1997; Boyd et al., 1999; Sedwick et al., 1999; Hutchins et al., 2001). It has also been documented that iron enrichment in the Ross Sea can lead to changes in phytoplankton community composition. Martin et al. (1990b) and Sedwick et al. (2000) reported that diatoms were favored by iron addition in comparison to other groups.

Our study observed a similar trend, in that both absolute diatom abundance and the diatom to *P. antarctica* ratio represented by the results of pigment analyses were significantly increased after iron enrichment. Iron additions also increased biogenic silica production, and led to higher nitrate and phosphate drawdown. Based on pump and probe fluorometry, it has been suggested that the growth of *P. antarctica* could also be iron limited in this area (Olson et al., 2000).

The shift to increased diatom relative abundance in the high-iron treatments may be partially explained by the higher photosynthetic capacity of diatoms and their greater iron affinity. These characteristics allow diatoms to efficiently utilize the micronutrients at lower concentrations (Sedwick et al., 2007). The decreased Fuco to Hex ratios in the high-light and control treatments are consistent with *Phaeocystis* having faster photorecovery mechanisms and a more resilient xanthophyll cycle as photoprotective mechanisms (Kropuenske et al., 2009). Photosynthetic responses indicated that the major response in the experiment was a strong acclimation to irradiance, as P^B_{max} and α values increased markedly. There was also a suggestion that increased iron concentrations resulted in greater P^B_{max} rates, and also possibly that α values were elevated under low light as a response to increased CO_2 (Table 2). However, given the low number of replicates within the *P–E* treatments, it is impossible to clearly determine the strength of this relationship.

F_v/F_m will reflect iron status, but it can also be impacted by light stress. Cells can take longer to reach an optimal F_v/F_m if they have been subjected to high light and are damaged from photoinhibition. This characteristic decline of F_v/F_m is consistently shown by our FRRF measurements, as low-light samples regularly reach higher values when compared to their high-light counterparts.

In our study the influence of iron on *P. antarctica* abundance was greatly magnified under high light, since the abundance of *Phaeocystis* colonies was almost doubled after iron enrichment under higher irradiance. However, this was not the case under low light, where colony abundance was much lower than under high light, regardless of iron availability. Shields and Smith (2009) found that colony growth rates were greater than those of solitary cells under light-saturating, nutrient-replete conditions, so that it is possible that the net effect in the high light treatment may have resulted from differential growth. This strong interactive effect of light and iron on the formation of *Phaeocystis* colonies is also consistent with laboratory studies using a recent Ross Sea isolate of *P. antarctica* (Sedwick et al., 2007). As discussed above, the formation of *Phaeocystis* colonies could confer a physiological advantage by acting as an extracellular reservoir of photosynthetically generated carbon or trace metals (Lancelot, 1983; Rousseau et al., 1994; Davidson and Marchant, 1987). This suggests that under low light, when photosynthesis is light-limited, colony formation could be limited by energy availability. When light is saturating, large amount of extracellular carbon (mucus) could be produced to form colonies. Because of the interactions between light and iron limitation (Sunda and Huntsman, 1997; Boyd et al., 1999, 2001), iron limitation of photosynthetic carbon fixation could have a similar effect on colony formation. Under suboptimal irradiances, the iron half-saturation constant for growth of cultured *P. antarctica* is increased (Garcia et al., 2009). In fact, our results strongly suggest that the process of colony formation was co-limited by both iron and light availability, again highlighting the importance of this dual limitation in the Ross Sea.

It has been suggested that macronutrient limitation promotes the dominance of the *Phaeocystis* flagellated single cell morphotype (Wassmann et al., 1990; Escaravage et al., 1995). Similarly, iron limitation may favor flagellated cells due to their relatively higher volume-normalized diffusional iron flux. When iron concentration is low, single cells may be more favored due to their relatively much greater surface to volume ratio; conversely, the colonial form may be more favored after iron enrichment. A study in the northern Humboldt Current offshore of Peru also observed that iron addition strongly promoted the switch of *P. globosa* flagellates to colonies (Hutchins et al., 2002). Due to the critical role that *P. antarctica* plays in the Ross Sea carbon cycle and the differential contribution to carbon export of the two *Phaeocystis* stages (Smith et al., 2003), this interactive effect of iron and light on the formation of colonies from solitary cells has important implications for biological carbon uptake in the Southern Ocean.

Another important result of this study was the dramatic increase in the relative abundance of the large, chain-forming centric diatom *Chaetoceros* over the small, solitary pennate diatom *Cylindrotheca* under elevated CO_2 concentration. Our results support the findings of Tortell et al. (2008), who also observed a similar switch from the pennate *Pseudo-nitzschia* to *Chaetoceros* under CO_2 enrichment in an iron-enriched Ross Sea

diatom assemblage. While this effect was observed under both low-light and high-light conditions, it was greatly enhanced at higher irradiance. In fact, diatom community structure was very responsive to all three variables we examined, with significant shifts resulting from changes in iron, light, and CO_2 individually, from every two-way combination, and from all three together (Table 3). Due to the differences of these two taxa in supporting potential carbon export (Stickley et al., 2005), any combination of environmental changes that favors the larger centric diatom group could increase vertical fluxes of organic carbon from Ross Sea surface waters.

Some of the most novel findings of our study were these interactive effects by the three parameters irradiance, iron, and CO_2. In general, light and iron together had a broad combined influence on overall phytoplankton community structure and elemental ratios. Light and CO_2, iron and CO_2, and all three variables in combination had more specific effects on the species composition and size structure of the diatom component of the assemblage. These interactive effects provide new evidence and insights to help understand how irradiance, iron, and CO_2 together may regulate Ross Sea phytoplankton community structure and biogeochemistry. In future global change scenarios, irradiance, iron supply, and CO_2 concentration will likely all change simultaneously (Boyd and Doney, 2002). Our study suggests that to fully understand the controls on present day Ross Sea phytoplankton communities and anticipate how they could change in the future, it is necessary to consider both the changes in all three factors individually, and in their more difficult-to-predict mutual interactions in combination.

Acknowledgments

This project was supported by NSF Grants ANT 0741411 and ANT 0741428 to D.A.H., ANT 0338157 to W.O.S., ANT 0338097 to G.R.D., ANT 0528715 to J.M.R., ANT 0338350 to R.B.D., and (NSFC) 40776093 40676089 to S.J.. The authors would like to thank Dr. Peter Sedwick for helping with clean seawater collections, Dr. Zbigniew Kolber for providing the bench-top MBARI Fast Repetition Rate Fluorometer, the crew and captain of the *RV/IB* Nathaniel B. Palmer, the science technicians and logistics support staff from Raytheon Polar Service, and three anonymous reviewers for their helpful comments.

References

Algina, J., Olejnik, S.F., 1984. Implementing the Welch–James procedure with factorial designs. Educational and Psychological Measurement 44, 39–48.

Alley, D., Berntsen, T., Bindoff, N.L., Chen, Z.L., Chidthaisong, A., Friedlingstein, P., Gregory, J., Hegerl, G., Heimann, M., Hewitson, B., Hoskins, B., Joos, F., Jouzel, J., Kattsov, V., Lohmann, U., Manning, M., Matsuno, T., Molina, M., Nicholls, N., Overpeck, J., Qin, D.H., Raga, G., Ramaswamy, V., Ren, J.W., Rusticucci, M., Solomon, S., Somerville, R.T., Stocker, F.P., Stott, P., Stouffer, R.J., Whetton, P., Wood, R.A., Wratt, D., 2007. Climate Change 2007: The physical science basis—summary for policymakers. Contribution of Working Group I to the Fourth Assessment Report of the Intergovernmental Panel on Climate Change, IPCC Secretariat.

Arrigo, K.R., DiTullio, G.R., Dunbar, R.B., Lizotte, M.P., Robinson, D.H., VanWoert, M., Worthen, D.L., 2000. Phytoplankton taxonomic variability and nutrient utilization and primary production in the Ross Sea. Journal of Geophysical Research 105, 8827–8846.

Arrigo, K.R., Robinson, D.H., Worthen, D.L., Dunbar, R.B., DiTullio, G.R., Van Woert, M., Lizotte, M.P., 1999. Phytoplankton community structure and the drawdown of nutrients and CO_2 in the Southern Ocean. Science 283, 365–367.

Bates, N.R., Hansell, D.A., Carlson, C.A., Gordon, L.I., 1998. Distribution of CO_2 species, estimates of net community production and air sea CO_2 exchange in the Ross Sea polynya. Journal of Geophysical Research 103, 2883–2896.

Blain, S., Sarthou, G., Laan, P., 2008. Distributions of dissolved iron during the natural iron fertilisation experiment KEOPS (Kerguelen Island, Southern Ocean). Deep-Sea Research II 55, 594–605.

Boyd, P.W., Abraham, E.R., 2001. Iron-mediated changes in phytoplankton photosynthetic competence during Soiree. Deep-Sea Research II 48, 2529–2550.

Boyd, P.W., Doney, S.C., 2002. Modelling regional responses by marine pelagic ecosystems to global climate change. Geophysical Research Letters 29, 531–534, doi:10.1029/2001GL014130.

Boyd, P.W., LaRoche, J., Gall, M., Frew, R., McKay, R.M.L., 1999. Role of iron, light, and silicate in controlling algal biomass in subantarctic waters SE of New Zealand. Journal of Geophysical Research 104, 13395–13408.

Boyd, P.W., Crossley, C., DiTullio, G.R., Griffiths, F.B., Hutchins, D.A., Queguiner, B., Sedwick, P.N., Trull, T.W., 2001. Control of phytoplankton growth by iron supply and irradiance in the subantarctic Southern Ocean: experimental results from the SAZ project. Journal of Geophysical Research 106, 31573–31583.

Boyd, P.W., Watson, A.J., Law, C.S., Abraham, E.R., Trul, T., Murdoch, R., Bakker, D.C., Bowie, A.R., Buesseler, K.O., Chang, H., Charette, M., Croot, P., Downing, K., Frew, R., Gall, M., Hadfield, M., Hall, J., Harvey, M., Jameson, G., LaRoche, J., Liddicoat, M., Ling, R., Maldonado, M.T., McKay, R.M., Nodder, S., Pickmere, S., Pridmore, R., Rintoul, S., Safi, K., Sutton, P., Strzepek, R., Tanneberger, K., Turner, S., Waite, A., Zeldis, J., 2000. A mesoscale phytoplankton bloom in the polar Southern Ocean stimulated by iron fertilization. Nature 407, 695–702.

Bruland, K.W., Rue, E.L., Smith, G.J., DiTullio, G.R., 2005. Iron, macronutrients and diatom blooms in the Peru Upwelling regime: brown and blue waters of Peru. Marine Chemistry 93, 81–103.

Brzezinski, M.A., Nelson, D.M., 1995. The annual silica cycle in the Sargasso Sea near Bermuda. Deep-Sea Research I 42, 1215–1237.

Buck, K.N., Lohan, M.C., Berger, C.J.M., Bruland, K.W., 2007. Dissolved iron speciation in two distinct river plumes and an estuary: implications for riverine iron supply. Limnology and Oceanography 52, 843–855.

Coale, K.H., Johnson, K.S., Chavez, F.P., Buesseler, K.O., Barber, R.T., Brzezinski, M.A., Cochlan, W.P., Millero, F.J., Falkowski, P.G., Bauer, J.E., Wanninkhof, R.H., Kudela, R.M., Altabet, M.A., Hales, B.E., Takahashi, T., Landry, M.R., Bidigare, R.R., Wang, X.J., Chase, Z., Strutton, P.G., Friederich, G.E., Gorbunov, M.Y., Lance, V.P., Hilting, A.K., Hiscock, M.R., Demarest, M., Hiscock, W.T., Sullivan, K.F., Tanner, S.J., Gordon, R.M., Hunter, C.N., Elrod, V.A., Fitzwater, S.E., Jones, J.L., Tozzi, S., Koblizek, M., Roberts, A.E., Herndon, J., Brewster, J., Ladizinsky, N., Smith, G., Cooper, D., Timothy, D., Brown, S.L., Selph, K.E., Sheridan, C.C., Twining, B.S., Johnson, Z.I., 2004. Southern ocean iron enrichment experiment: carbon cycling in high- and low-Si waters. Science 304, 408–414.

Coale, K.H., Wang, X., Tanner, S.J., Johnson, K.S., 2003. Phytoplankton growth and biological response to iron and zinc addition in the Ross Sea and Antarctic Circumpolar Current along 170°W. Deep-Sea Research II 50, 635–653.

de Baar, H.J.W., Buma, A.G.J., Nolting, R.F., Cadee, G.C., Jacques, G., Treguer, P.J., 1990. On iron limitation of the Southern Ocean: experimental observations in the Weddell and Scotia Seas. Marine Ecology Progress Series 65, 105–122.

de Baar, H.J.W., Boyd, P.W., Coale, K.H., Landry, M.R., Tsuda, A., Assmy, P., Bakker, D.C.E., Bozec, Y., Barver, R.T., Brezezinski, M.A., Buesseler, K.O., Boye, M., Croot, P.L., Gervais, F., Gorvunov, M.Y., Harrison, P.J., Hiscock, W.T., Laan, P., Lacelot, C., Law, C.S., Levasseur, M., Marchetti, A., Millero, F.J., Nishioka, J., Nojiri, Y., Van Oijen, T., Rievesell, U., Rijikenverg, M.J.A., Saito, H., Takeda, S., Timmermans, K.R., Veldhuis, M.J.W., Waite, A.M., Wong, C.-S., 2005. Synthesis of iron fertilization experiments: from the Iron Age to the Age of Enlightenment. Journal of Geophysical Research 110, C09S16, doi:10.1029/2004JC002601.

Davidson, A.T., Marchant, H.J., 1987. Binding of manganese by Antarctic *Phaeocystis pouchetii* and the role of bacteria in its release. Marine Biology 95, 481–487.

Dickson, A.G., Afghan, J.D., Anderson, G.C., 2003. Reference materials for oceanic CO_2 analysis: a method for the certification of total alkalinity. Marine Chemistry 80, 185–197.

DiTullio, G.R., Garcia, N.S., Riseman, S.F., Sedwick, P.N., 2007. Effects of iron concentration on the pigment composition of *Phaeocystis antarctica* in the Ross Sea at low irradiance. Biogeochemistry 83, 71–81.

DiTullio, G.R., Geesey, M.E., 2002. Photosynthetic pigments in marine algae and bacteria. In: Bitton, G. (Ed.), The Encyclopedia of Environmental Microbiology. John Wiley & Sons Inc.,, New York, pp. 2453–2470.

DiTullio, G.R., Grebmeier, J.M., Arrigo, K.R., Lizotte, M.P., Robinson, D.H., Leventer, A., Barry, J.P., VanWoert, M.L., Dunbar, R.B., 2000. Rapid and early export of *Phaeocystis antarctica* blooms in the Ross Sea, Antarctica. Nature 404, 595–598.

DiTullio, G.R., Smith Jr., W.O., 1995. Relationship between dimethylsulfide and phytoplankton pigment concentrations in the Ross Sea, Antarctica. Deep-Sea Research I 42, 873–892.

DiTullio, G.R., Smith Jr., W.O., 1996. Spatial patterns in phytoplankton biomass and pigment distributions in the Ross Sea. Journal of Geophysical Research 101, 18467–18477.

Dickson, A.G., Goyet, C. (Eds.), 1994. DOE, Handbook of Methods for the Analysis of the Various Parameters of the Carbon Dioxide System in Sea Water. Version 2, ORNL/CDIAC-74.

Dunbar, R.B., Arrigo, K.R., DiTullio, G.D., Leventer, A., Lizotte, M.P.m, Van Woert, M.L., Robinson, D.H., 2003. Non-Redfield production and export of marine organic matter: a recurrent part of the annual cycle in the Ross Sea, Antarctica. In: DiTullio, G., Dunbar, R. (Eds.), Biogeochemistry of the Ross Sea, American Geophysical Union, vol. 78. Antarctic Research Series Monograph, pp. 179–196.

Escaravage, V., Peperzak, L., Prins, T.C., Peters, J.C., Joordens, J.C., 1995. The development of a *Phaeocystis* bloom in a mesocosm experiment in relation to nutrients, irradiance and coexisting algae. Ophelia 42, 55–74.

Feng, Y., Warner, M.E., Zhang, Y., Sun, J., Fu, F.-X., Rose, J.M., Hutchins, D.A., 2008. Interactive effects of increased pCO_2, temperature and irradiance on the marine coccolithophore *Emiliania huxleyi* (Prymnesiophyceae). European Journal of Phycology 43, 87–98.

Feng, Y., Hare, C.E., Leblanc, K., Rose, J.M., Zhang, Y., DiTullio, G.R., Lee, P.A., Wilhelm, S.W., Rowe, J.M., Sun, J., Nemcek, N., Gueguen, C., Passow, U., Benner, I., Brown, C., Hutchins, D.A., 2009. Effects of increased pCO_2 and temperature on the North Atlantic spring bloom. I. The phytoplankton community and biogeochemical response. Marine Ecology Progress Series 388, 13–25.

Firme, G.F., Rue, E.L., Weeks, D.A., Bruland, K.W., Hutchins, D.A., 2003. Spatial and temporal variability in phytoplankton iron limitation along the California coast and consequences for Si, N, and C biogeochemistry. Global Biogeochemical Cycles 17, 1016 doi: 10.1029/2001GB001824.

Franck, V.M., Bruland, K.W., Hutchins, D.A.., Brzezinski, M.A., 2003. Fe and Zn effects on silicic acid and nitrate uptake kinetics in three high-nutrient, low chlorophyll (HNLC) regions. Marine Ecology Progress Series 252, 15–33.

Fu, F.-X., Mulholland, M.R., Garcia, N., Beck, A., Bernhardt, P.W., Warner, M.E., Sañudo-Wilhelmy, S.A., Hutchins, D.A., 2008. Interactions between changing pCO_2, N_2 fixation, and Fe limitation in the marine unicellular cyanobacterium *Crocosphaera*. Limnology and Oceanography 53, 2472–2484.

Garcia, N.S., Sedwick, P.N., DiTullio, G.R., 2009. Influence of irradiance and iron on the growth of colonial *Phaeocystis antarctica*: implications for seasonal bloom dynamics in the Ross Sea, Antarctica. Aquatic Microbial Ecology 57, 203–220.

Genty, B., Briantais, J.M., Baker, N.R., 1989. The relationship between the quantum yield of photosynthetic electron transport and quenching of chlorophyll fluorescence. Biochimica et Biophysica Acta 990, 87–92.

Gervais, F., Riebesell, U., Gorbunov, M.Y., 2002. Changes in primary productivity and chlorophyll a in response to iron fertilization in the Southern Polar Frontal Zone. Limnology and Oceanography 47, 1324–1335.

Gibson, J.A.E., Garrick, R.C., Burton, H.R., McTaggart, A.R., 1990. Dimethylsulfide and the alga *Phaeocystis pouchetti* in Antarctic coastal waters. Marine Biology 104, 339–346.

Gordon, L.I., Jennings, J.C., Ross, A.A., Krest, J.M., 1993. A Suggested Protocol for Flow Automated Analysis of Seawater Nutrients, WOCE Hydrographic Program Office, Methods Manual WHPO 91-1.

Haberman, K.L., Quetin, L.B., Ross, R.M., 2003a. Diet of the Antarctic krill (*Euphausia superba Dana*): I. Comparisons of grazing on *Phaeocystis antarctic*a (Karsten) and *Thalassiosira antarctica* (Comber). Journal of Experimental Marine Biology and Ecology 283, 79–95.

Haberman, K.L., Ross, R.M., Quetin, L.B., 2003b. Diet of the Antarctic krill (*Euphausia superba* Dana): II. Selective grazing in mixed phytoplankton assemblages. Journal of Experimental Marine Biology and Ecology 283, 97–113.

Hare, C.E., DiTullio, G.R., Trick, C.G., Wilhelm, S.W., Bruland, K.W., Rue, E.L., Hutchins, D.A., 2005. Phytoplankton community structure changes following simulated upwelled iron inputs in the Peru Upwelling region. Aquatic Microbial Ecology 38, 269–282.

Hare, C.E., DiTullio, G.R., Riseman, S.F., Crossley, A.C., Popels, L.C., Sedwick, P.N., Hutchins, D.A., 2007a. Effects of changing continuous iron input rates on a Southern Ocean algal assemblage. Deep-Sea Research I 54, 732–746.

Hare, C.E., Leblanc, K., DiTullio, G.R., Kudela, R.M., Zhang, Y., Lee, P.A., Riseman, S., Tortell, P.D., Hutchins, D.A., 2007b. Consequences of increased temperature and CO_2 for algal community structure and biogeochemistry in the Bering Sea. Marine Ecology Progress Series 352, 9–16.

Hewes, C.D., Reiss, C.S., Kahru, M., Mitchell, B.G., Holm-Hansen, O., 2008. Control of phytoplankton biomass by dilution and mixed layer depth in the western Weddell-Scotia Confluence. Marine Ecology Progress Series 366, 15–29.

Hopkinson, B.M., Barbeau, K.A., 2008. Interactive influences of iron and light limitation on phytoplankton at subsurface chlorophyll maxima in the eastern North Pacific. Limnology and Oceanography 53, 1303–1318.

Hutchins, D.A., Bruland, K.W., 1998. Iron-limited diatom growth and Si:N uptake ratios in a coastal upwelling regime. Nature 393, 561–564.

Hutchins, D.A., DiTullio, G.R., Zhang, Y., Bruland, K.W., 1998. An iron limitation mosaic in the California upwelling regime. Limnology and Oceanography 43, 1037–1054.

Hutchins, D.A., Hare, C.E., Pustizzi, F.P., Trick, C.G., DiTullio, G.R., 2003. A shipboard natural community continuous culture system to examine effects of low-level nutrient enrichments on phytoplankton community composition. Limnology and Oceanography Methods 1, 82–91.

Hutchins, D.A., Hare, C.E., Weaver, R.S., Zhang, Y., Firme, G.F., Ditullio, G.R., Aim, M.B., Riseman, S.F., Maucher, J.M., Geesey, M.E., Trick, C.G., Smith, G.J., Rue, E.L., Conn, J., Bruland, K.W., 2002. Phytoplankton iron limitation in the Humbolt Current and Peru Upwelling. Limnology and Oceanography 47, 997–1011.

Hutchins, D.A., Sedwick, P.N., Ditullio, G.R., Boyd, P.W., Queguiner, B., Griffiths, F.B., Crossley, C., 2001. Control of phytoplankton growth by iron and silicic acid availability in the subantarctic Southern Ocean: experimental results from the SAZ Project. Journal of Geophysical Research 106, 31559–31572.

Ishii, M., Inoue, H.Y., Matsueda, H., Tanoue, E., 1998. Close coupling between seasonal biological production and dynamics of dissolved inorganic carbon in the Indian Ocean sector and the western Pacific Ocean sector of the Antarctic Ocean. Deep-Sea Research 45, 1187–1209.

Janse, I., van Rijssel, M., Gottschal, J.C., Lancelot, C., Gieskes, W.W.C., 1996. Carbohydrates in the North Sea during spring blooms of *Phaeocystis*: a specific fingerprint. Aquatic Microbial Ecology 10, 97–103.

Jennings Jr., J.C., Gordon, L.I., Nelson, D.M., 1984. Nutrient depletion indicates high primary productivity in the Weddell Sea. Nature 309, 51–54.

Karl, D.M., Tilbrook, B.D., Tien, G., 1991. Seasonal coupling of organic matter production and particle flux in the western Bransfield Strait, Antarctica. Deep-Sea Research 38, 1097–1126.

Kinnaer, P.R., Gray, C.D., 1997. SPSS for Windows Made Simple, second ed. Psychology Press, Hove UK.

Knox, G.A., 1994. The Biology of the Southern Ocean. Cambridge University Press, New York. ISBN O-52 l-322 1 l-1, 444pp.

Kolber, Z.S., Barber, R.T., Coale, K.H., Fitzwater, S.E., Greene, R.H., Johnson, K.S., Lindley, S., Falkowski, P.G., 1994. Iron limitation of phytoplankton photosynthesis in the equatorial Pacific Ocean. Nature 7, 145–149.

Kropuenske, L.R., van Dijken, G.L., Mills, M.M., Robinson, D.H., Arrigo, K.R., 2009. Photophysiology in two major Southern Ocean phytoplankton taxa: photoprotection in *Phaeocystis antarctica* and *Fragilariopsis cylindrus*. Limnology and Oceanography 54, 1176–1196.

Lancelot, C., 1983. Metabolic changes in *Phaeocystis pouchetii* (Hariot) Lagerheim during the spring bloom in Belgian coastal waters. Estuarine, Coastal, and Shelf Science 18, 593–600.

Lancelot, C., Mathot, S., 1985. Biochemical fractionation of primary production by phytoplankton in Belgian coastal waters during short and long term incubations with ^{14}C bicarbonate. II. *Phaeocystis pouchetii* colonial population. Marine Biology 86, 227–232.

Leblanc, K., Hare, C.E., Boyd, P.W., Bruland, K.W., Sohst, B., Pickmere, S., Lohan, M.C., Buck, K., Ellwood, M., Hutchins, D.A., 2005. Fe and Zn effects on the Si cycle and diatom community structure in two contrasting high and low-silicate HNLC areas. Deep-Sea Research I 52, 1842–1864.

Lohan, M.C., Statham, P.J., Crawford, D.W., 2002. Total dissolved zinc in the upper water column of the subarctic north east Pacific. Deep Sea Research II 49, 5793–5808.

Lovenduski, N.S., Gruber, N., 2005. The impact of the Southern Annular Mode on Southern Ocean circulation and biology. Geophysical Research Letters 32, L11603, doi:10.1029/2005GL022727.

Martin, J.H., Fitzwater, S.E., Gordon, R.M., 1990a. Iron deficiency limits phytoplankton growth in Antarctic waters. Global Biogeochemical Cycles 4, 5–12.

Martin, J.H., Gordon, R.M., Fitzwater, S.E., 1990b. Iron in Antarctic waters. Nature 345, 156–158.

Mathot, S., Smith, W.O., Carlson, C.A., Garrison, D.L., Gowing, M.M., Vickers, C.L., 2000. Carbon partitioning within *Phaeocystis antarctica* (Prymnesiophyceae) colonies in the Ross Sea, Antarctica. Journal of Phycology 36, 1049–1056.

Mehrbach, ., Culberson, C.H., Hawley, J.E., Pytkowicz, R.M., 1973. Measurement of the apparent dissociation constants of carbonic acid in seawater at atmospheric pressure. Limnology and Oceanography 18, 897–907.

Mitchell, B.G., Holm-Hansen, O., 1991. Observations and modeling of the Antarctic phytoplankton crop in relation to mixing depth. Deep-Sea Research 38, 981–1007.

Moisan, T.A., Mitchell, B.G., 1999. Photophysiological acclimation of *Phaeocystis antarctica* Karsten under light limitation. Limnology and Oceanography 44, 247–258.

Moisan, T.A., Olaizola, M., Mitchell, B.G., 1998. Xanthophyll cycling in *Phaeocystis antarctica*: changes in cellular fluorescence. Marine Ecology Progress Series 169, 113–121.

Montes-Hugo, M., Doney, S.C., Ducklow, H.W., Fraser, W., Martinson, D., Stammerjohn, S.E., Schofield, O., 2009. Recent changes in phytoplankton communities associated with rapid regional climate change along the western Antarctic Peninsula. Science 323, 1470–1473.

Nelson, D.M., Smith Jr., W.O., 1991. Sverdrup revisited: critical depths, maximum chlorophyll levels, and the control of Southern Ocean productivity by the irradiance-mixing regime. Limnology and Oceanography 36, 1650–1661.

Nodder, S.D., Charette, M.A., Waite, A.M., Trull, T.W., Boyd, P.W., Zeldis, J., Buesseler, K.O., 2001. Particle transformations and export flux during an in situ iron stimulated algal bloom in the Southern Ocean. Geophysical Research Letters 28, 2409–2412.

Olson, R.J., Sosik, H.M., Chekalyuk, A.M., Shalapyonok, A., 2000. Effects of iron enrichment on phytoplankton in the Southern Ocean during late summer: active fluorescence and flow cytometric analyses. Deep-Sea Research II 47, 3181–3200.

Palmisano, A.C., SooHoo, J.B., SooHoo, S.L., Kottmeier, S.T., Craft, L.L., Sullivan, C.W., et al., 1986. Photoadaptation in *Phaeocystis pouchetii* advected beneath annual sea ice in McMurdo Sound, Antarctica. Journal of Plankton Research 8, 891–906.

Peloquin, J.A., Smith Jr., W.O., 2007. Phytoplankton blooms in the Ross Sea, Antarctica: interannual variability in magnitude, temporal patterns, and composition. Journal of Geophysical Research 112, C08013, doi:10.1029/2006JC003816.

Pickell, L.D., Wells, M.L., Trick, C.G., Cochlan, W.P., 2009. A sea-going continuous culture system for investigating phytoplankton community response to macro- and micro-nutrient (trace metal) manipulations. Limnology and Oceanography Methods 7, 21–32.

Platt, T., Harrison, W.G., 1980. Photoinhibition of photosynthesis in natural assemblages of marine phytoplankton. Journal of Marine Research 38, 687–701.

Pollard, R.T., Salter, I., Sanders, R.J., Lucas, M.I., Moore, C.M., Mills, R.A., Statham, P.J., Allen, J.T., Baker, A.R., Bakker, D.C.E., Charette, M.A., Fielding, S., Fones, G.R., French, M., Hickman, A.E., Holland, R.J., Hughes, J.A., Jickells, T.D., Lampitt, R.S., Morris, P.J., Nédélec, F.H., Nielsdóttir, M., Planquette, H., Popova, E.E., Poulton, A.J., Read, J.F., Seeyave, S., Smith, T., Stinchcombe, M., Taylor, S., Thomalla, S.,

Venables, J.L., Williamson, R., Zubkov, M.V., 2009. Southern Ocean deep-water carbon export enhanced by natural iron fertilization. Nature 457, 577–580.
Riebesell, U., 2004. Effects of CO_2 enrichment on marine phytoplankton. Journal of Oceanography 60, 719–729.
Robinson, D.H., Arrigo, K.R., Lizotte, M., DiTullio, G.R., 2003. Evaluating phytoplankton productivity in waters dominated by *Phaeocystis antarctica*. In: DiTullio, G.D., Dunbar, R.B. (Eds.), Biogeochemistry of the Ross Sea. American Geophysical Union, Washington, DC.
Rousseau, V., Vaulot, D., Casotti, R., Cariou, V., Lenz, J., Gunkel, J., Baumann, M., 1994. The life cycle of *Phaeocystis* (Prymnesiophyceae): evidence and hypotheses. Journal of Marine Systems 5, 23–39.
Rousseeuw, P.J., van Zomeren, B.C., 1990. Unmasking multivariate outliers and leverage points. Journal of the American Statistical Association 85, 633–639.
Rubin, S.I., Takahashi, T., Chipman, D.W., Goddard, J.G., 1998. Primary productivity and nutrient utilization ratios in the pacific sector of the southern ocean based on seasonal changes in seawater chemistry. Deep-Sea Research II 45, 1211–1234.
Sarmiento, J.L., Hughes, T.M.C., Stouffer, R.J., Manabe, S., 1998. Simulated response of the ocean carbon cycle to anthropogenic climate warming. Nature 393, 245–249.
Sarmiento, J.L., Toggweiler, J.L., 1984. A new model for the role of the oceans in determining atmospheric pCO_2. Nature 308, 621–624.
Scharek, R., van Leeuwe, M.A., de Baar, H.J.W., 1997. Responses of Southern Ocean phytoplankton to the addition of trace metals. Deep-Sea Research II 44, 209–227.
Scott, F.J., Marchant, H.J. (Eds.), 2005. Antarctic Marine Protists. Australian Biological Resources Study. Canberra and Australian Antarctic Division, Hobart, pp. 13–201.
Sedwick, P.N., DiTullio, G.R., 1997. Regulation of algal blooms in Antarctic shelf waters by the release of iron from melting sea ice. Geophysical Research Letters 24, 2515–2518.
Sedwick, P.N., Garcia, N., Riseman, S.F., Marsay, C.M., DiTullio, G.R., 2007. Evidence for high iron requirements of colonial *Phaeocystis antarctica* at low irradiance. Biogeochemistry 83, 83–97.
Sedwick, P.N., Bowie, A.R., Trull, T.W., 2008. Dissolved iron in the Australian sector of the Southern Ocean (CLIVAR-SR3 section): Meridional and seasonal trends. Deep-Sea Research I, doi:10.1016/j.dsr.2008.03.011.
Sedwick, P.N., DiTullio, G.R., Hutchins, D.A., Boyd, P.W., Griffiths, F.B., Crossley, A.C., Trull, T.W., Quéguiner, B., 1999. Limitations of algal growth by iron deficiency in the Australian Subantarctic region. Geophysical Research Letters 26, 2865–2868.
Sedwick, P.N., DiTullio, G.R., Mackey, D.J., 2000. Iron and manganese in the Ross Sea, Antarctica: seasonal iron limitation in Antarctic shelf waters. Journal of Geophysical Research 105, 11321–11336.
Shields, A.R., Smith Jr., W.O., 2009. Size-fractionated photosynthesis/irradiance relationships during *Phaeocystis*-dominated blooms in the Ross Sea, Antarctica. Journal of Plankton Research 31, 701–712.
Smetacek, V., Nicol, S., 2005. Polar ocean ecosystems in a changing world. Nature 437, 362–368.
Smith Jr., W.O., Dennett, M.R., Mathot, S., Caron, D.A., 2003. The temporal dynamics of the flagellated and colonial stages of *Phaeocystis antarctica* in the Ross Sea. Deep-Sea Research II 50, 605–617.
Smith Jr., W.O., Asper, V.L., 2001. Spatial and temporal variations in phytoplankton: biomass in the Ross Sea polynya. Deep-Sea Research I 48, 137–161.
Smith Jr., W.O., Nelson, D.M., 1985. Phytoplankton bloom produced by a receding ice edge in the Ross Sea: spatial coherence with the density field. Science 227, 163–166.
Smith Jr., W.O., Marra, J., Hiscock, M.R., Barber, R.T., 2000. The seasonal cycle of phytoplankton biomass and primary productivity in the Ross Sea, Antarctica. Deep-Sea Research II 47, 3119–3140.
Solozano, L., Sharp, J.H., 1980. Determination of total dissolved phosphorus and particulate phosphorus in natural waters. Limnology and Oceanography 25, 756–760.
Sournia, A., 1986. Atlas du phytoplancton marin Paris (France): CNRS, 3 volumes.
Steig, E.J., Schneider, D.P., Rutherford, S.D., Mann, M.E., Comiso, J.C., Shindell, D.T., 2009. Warming of the Antarctic ice-sheet surface since the 1957 International Geophysical Year. Nature 457, 459–462.
Stickley, C.E., Pike, J., Leventer, A., Dunbar, R., Domack, E.W., Brachfeld, S., Manley, P., McClennan, C., 2005. Deglacial ocean and climate seasonality in laminated diatom sediments, MacRobertson Shelf, Antarctica. Palaeogeography, Palaeoclimatology, Palaeoecology 227, 290–310.
Strass, V.H., 2002. Eisen-Ex-1: test of the iron hypothesis in a Southern Ocean eddy, Eos Transactions AGU, 83, Abstract OS26.
Strzepek, R.F., Harrison, P.J., 2004. Photosynthetic architecture differs in coastal and oceanic diatoms. Nature 431, 689–692.
Sun, J., Qian, S.B., 2002. A quantitative research and analysis methods for marine phytoplankton: an introduction to Utermöhl method and its modification. Journal of Oceanography, Huanghai Bohai Seas 20, 105–112.
Sunda, W.G., Huntsman, S.A., 1995. Iron uptake and growth limitation in oceanic and coastal phytoplankton. Marine Chemistry 50, 189–206.
Sunda, W.G., Huntsman, S.A., 1997. Interrelated influence of iron, light and cell size on marine phytoplankton growth. Nature 390, 389–392.
Sweeney, C., Hansell, D.A., Carlson, C.A., Codispoti, L.A., Gordon, L.I., Marra, J., Millero, F.J., Smith Jr., W.O., Takahashi, T., 2000. Biogeochemical regimes, net community production and carbon export in the Ross Sea, Antarctica. Deep-Sea Research II 47, 3369–3394.
Takeda, S., 1998. Influence of iron availability on nutrient consumption ratio of diatoms in oceanic waters. Nature 393, 774–777.
Timmermans, K.R., Gerringa, L.J.A., de Baar, H.J.W., van der Wagt, B., Veldhuis, M.J.W., de Jong, J.T.M., Croot, P.L., 2001. Growth rates of large and small Southern Ocean diatoms in relation to availability of iron in natural seawater. Limnology and Oceanography 46, 260–266.
Tomas, C.R., 1997. Identifying Marine Phytoplankton. Academic Press, New York.
Tortell, P.D., DiTullio, G.R., Sigman, D.M., Morel, F.M.M., 2002. CO_2 effects on taxonomic composition and nutrient utilization in an Equatorial Pacific phytoplankton assemblage. Marine Ecology Progress Series 236, 37–43.
Tortell, P.D., Payne, C.D., Li, Y., Trimborn, S., Rost, B., Smith, W.O., Riesselman, C., Dunbar, R.B., Sedwick, P., DiTullio, G.R., 2008. CO_2 sensitivity of Southern Ocean phytoplankton. Geophysical Research Letters 35, L04605, doi:10.1029/2007GL032583.
Tréguer, P., Nelson, D.M., Van Bennekom, A.J., DeMaster, D.J., Leynaert, A., Quéguiner, B., 1995. The silica balance in the world ocean: a reestimate. Science 268, 375–379.
Utermöhl, H., 1958. Zur Vervollkommnung der quantitativen Phytoplankton-Methodik Mitteilungen Internationale Vereinigung Theoretische und Angewandte. Limnologie 9, 1–38.
van Hilst, C.M., Smith Jr., W.O., 2002. Photosynthesis/irradiance relationships in the Ross Sea, Antarctica and their control by phytoplankton assemblage composition and environmental factors. Marine Ecology Progress Series 226, 1–12.
Vaughan, D.G., Gareth, J., Marshall, W.M., Connolley, C.P., Mulvaney, R., Hodgson, D.A., King, J.C., Pudsey, C.J., Turner, J., 2003. Recent rapid regional climate warming on the Antarctic Peninsula Climate Change 60, 243–274.
van Leeuwe, M.A., Stefels, J., 1998. Effects of iron and light stress on the biochemical composition of Antarctic *Phaeocystis* sp. (Prymnesiophyceae). II. Pigment composition. Journal of Phycology 34, 496–503.
Veldkamp, H., 1976. Continuous Culture in Microbial Physology and Ecology. Meadowfield Press Ltd., Durham p.68.
Verity, P.G., Smetacek, V., 1996. Organism life cycles, predation, and the structure of marine pelagic ecosystems. Marine Ecology Progress Series 130, 277–293.
Wassmann, P., Vernet, M., Mitchell, B.G., 1990. Mass sedimentation of *Phaeocystis pouchetii* in the Barents Sea. Marine Ecology Progress Series 66, 183–195.
Webb, W.L., Newton, M., Starr, D., 1974. Carbon dioxide exchange of *Alnus rubra*: a mathematical model. Oecologia 17, 28l–291.
Weiss, R.F., 1974. Carbon dioxide in water and seawater: the solubility of a non-ideal gas. Marine Chemistry 2, 203–215.
Welschmeyer, N.A., 1994. Fluorometric analysis of chlorophyll a in the presence of chlorophyll b and pheopigments. Limnology and Oceanography 39, 1985–1992.
Wilcox, R.R., 1997. Introduction to Robust Estimation and Hypothesis Testing. Academic Press, San Diego, pp. 296.
Wilcox, R.R., 2003. Applying Contemporary Statistical Techniques. Academic Press, New York, USA.
Zapata, M., Rodriguez, F., Garrido, J.L., 2000. Separation of chlorophylls and carotenoids from marine phytoplankton: a new HPLC method using a reversed phase C_8 column and pyridine-containing mobile phases. Marine Ecology Progress Series 195, 29–45.